THESIS FOR THE DEGREE OF DOCTOR OF PHILOSOPHY

Development of voyage optimization algorithms for sustainable shipping and their impact to ship design

HELONG WANG

Department of Mechanics and Maritime Sciences

CHALMERS UNIVERSITY OF TECHNOLOGY

Gothenburg, Sweden 2020

Development of voyage optimization algorithms for sustainable shipping and their impact to ship design
HELONG WANG
ISBN 978-91-7905-259-1

Doktorsavhandlingar vid Chalmers tekniska högskola
Ny serie nr 4726
ISSN 0346-718X

Department of Mechanics and Maritime Sciences
Chalmers University of Technology
SE-412 96 Gothenburg
Sweden
Telephone + 46 (0)31-772 1000

Printed by Chalmers Reproservice, Chalmers University of Technology
Gothenburg, Sweden 2020

Development of voyage optimization algorithms for sustainable shipping and their impact to ship design

HELONG WANG
Division of Marine Technology
Department of Mechanics and Maritime Sciences
Chalmers University of Technology

Abstract

The environmental impacts from shipping and the societal challenges of human and property losses caused by ship accidents are pressuring the shipping industry to improve its energy efficiency and enhance ship safety. Voyage optimization is such an effective measure that has been widely adopted in today's shipping market. The voyage optimization algorithm is the dominant part of any voyage optimization methods. The main objective of this thesis is to develop sophisticated voyage optimization algorithms, explore their applications to sustainable ship operations, and study its impact on ship fatigue design.

In this thesis, five commonly used voyage optimization algorithms are first implemented and compared to provide a foundation for understanding optimization algorithms. A three-dimensional Dijkstra's algorithm is then developed with further improvement based on the comparison. It can provide globally optimal solutions and conducting multi-objective voyage optimization. An engine-power based multi-objective optimization algorithm is proposed for the aid of ship operations with power-setting in their navigation system. Furthermore, the influence of the uncertainties from voyage optimization inputs, e.g., metocean forecast, implemented ship performance models and voyage optimization algorithms, on the optimization results is investigated. Moreover, the capabilities of the proposed voyage optimization algorithms to handle other optimization objectives, i.e., less fatigue damage accumulation and lower fatigue crack propagation rate, is also investigated. Meanwhile, two statistical wave models are compared to study the variation of a ship's encountered wave environment for ship fatigue design. The impact of voyage optimization aided operations on a ship's encountered wave environments and fatigue life assessment is also researched in this thesis.

The three-dimensional Dijkstra's algorithm addresses the limitations of conventional voyage optimization algorithms and allows for voluntary speed variation. It has a great potential of saving fuel up to about 12% in comparison with the case study ship's actual sailing routes. The ship engine setting-based optimization algorithm provides a scheme based on a genetic algorithm and dynamic programming concept. It has the potential to save fuel up to approximately 14.5% compared to the actual sailing routes. This study also shows that metocean uncertainties in the voyage optimization process have great influence on the optimization results, i.e., 3-10% difference in fuel consumption for the same voyage optimization method. In addition, statistical wave models have been proven to capture ship-encountered wave statistics. It is also shown that the actual wave environments encountered by ships differ significantly from the wave scatter diagram provided by class guidelines. A good voyage optimization method can help to extend a ship's fatigue life by at least 50%.

Keywords: Dijkstra's algorithm; Energy efficiency; Expected time of arrival (ETA); Genetic algorithm; Metocean forecast; Ship safety; Sustainable shipping; Voyage optimization algorithms.

Preface

This thesis is composed of the research work performed at the Division of Marine Technology, Department of Mechanics and Maritime Science at Chalmers University of Technology, from June 2016 to May 2020. The work is funded by the EU Horizon2020 Earth Observation for Maritime Navigation (EONav, GA no. 687537) and co-friendly and customer-driven Sail plan optimization service (EcoSail, GA no. 820593) projects.

Thanks to:

- My supervisor Wengang Mao and co-supervisor Leif Eriksson for good discussion and support.
- My examiner and co-supervisor Jonas W. Ringsberg for making our division a good place to work and leading us forward.
- My colleagues at the Division of Marine Technology for all their support.
- My family for their support.

Finally, I would like to express my appreciation once again to my main supervisor, Wengang Mao, for all the dedicated support in my studies, work and life.

Gothenburg, April 2020

Helong Wang

Contents

List of appended papers

For appended papers **A-E**, the author of this thesis contributed to the ideas presented, planned the contents of the papers with the coauthors, did most of the programming and wrote most of the manuscript. In **Paper F**, the author did the part of the analysis and data postprocessing. In **Paper G**, the author was involved in the code development, actual analysis, data pre- and post-processing, as well as writing part of the paper.

Paper A Wang, H., Mao, W., and Eriksson, L. (2017). Benchmark study of five optimization algorithms for weather routing. Proceedings of the ASME 2017 36th International Conference on Ocean, Offshore and Arctic Engineering (OMAE2017) in Trondheim, Norway, June 25-30, 2017. OMAE2017-61022.

Paper B Wang, H., Mao, W., and Eriksson, L. (2019). A three-dimensional Dijkstra's algorithm for multi-objective ship voyage optimization. Ocean Engineering, 186(1), 106131. DOI: 10.1016/j.oceaneng.2019.10613.

Paper C Wang, H., Lang, X., and Mao, W. (2019). A ship engine power-based voyage optimization method by combing genetic algorithm and dynamic programming concepts. (Submitted for journal publication, under review.)

Paper D Wang, H., Lang, X., Mao, W., Zhang, D., and Storhaug, G. (2020). Effectiveness of 2D optimization algorithms considering voluntary speed reduction under uncertain metocean conditions. Ocean Engineering, 200(1), 107063. DOI: 10.1016/j.oceaneng.2020.107063.

Paper E Wang, H., Mao, W., and Zhang, D. (2019). Voyage optimization for mitigating ship structural failure due to crack propagation. Journal of Risk and Reliability, 233(1), pp. 5-17. DOI: 10.1177/1748006X18754976.

Paper F De Gracia, L., Wang, H., Mao, W., Osawa, N., and Rychlik, I. (2019). Comparison of two statistical wave models for fatigue and fracture analysis of ship structures. Ocean Engineering, 187(1), 106161. DOI: 10.1016/j.oceaneng.2019.106161.

Paper G Lang, X., Wang, H., Mao, W., and Osawa, N. (2020). Impact of voyage optimizations aided operation on a ship's fatigue design. (Submitted for journal publication, under review.)

List of other published papers by the author

For other published papers **II** and **III**, the author of this thesis contributed to the ideas presented, planned the contents of the papers with the coauthors, did most of the programming and wrote most of the manuscript. In **Paper I**, the author did the part of the data postprocessing.

Paper I Eriksson, L., Ye, Y., Jonasson, L., Qazi, W., Mao, W., Wang, H., Möller, J., Lemmens, K., and Dokken, S. (2018). EONav – Copernicus data in support of maritime route optimization. Proceedings of the 2018 International Geoscience and Remote Sensing Symposium (IGARSS 2018) in Valencia, Spain, July 22-27, 2018, pp. 5606-5609. DOI: 10.1109/IGARSS.2018.8519477

Paper II Wang, H., Mao, W., and Eriksson, L. (2018). MetOcean data drived voyage optimization using genetic algorithm. Proceedings of the 28th International Society of Offshore and Polar Engineers (ISOPE 2018) in Sapporo, Japan, June 8-13, 2018, ISOPE-I-18-283, pp. 697-705.

Paper III Wang, H., Mao, W., and Eriksson, L. (2019). Efficiency of a voluntary speed reduction algorithm for a ship's great circle sailing. Proceedings of the 13th International Conference on Marine Navigation and Safety of Sea Transportation, Gdańsk, Poland, June 11-13, 2019.

Nomenclature

Roman letters

a	Crack length [mm]
$\boldsymbol{A}$	Edge set of a graph
A_{XV}	Transverse projected area above the waterline including superstructures [m^2]
c_{sfoc}	Specific fuel oil consumption [g/kwh]
C_u, C_v	Current velocity towards the east and the north, respectively [m/s]
C_{AA}	Wind resistance coefficient; $C_{AA}(0)$ means the wind resistance coefficient in head wind
$\boldsymbol{C}(\boldsymbol{P}, \boldsymbol{U}(\boldsymbol{P}))$	Ship sailing constraints
D	Accumulated damage
D_T	Expected fatigue damage caused by the narrow band stress
$\boldsymbol{D}$	Decision vector
f_{ic}	Instantaneous cost function
$f\left(\frac{a}{w}\right)$	A dimensionless parameter in terms of the crack geometry and type of loading
$f_s(s)$	Probability density function of stress cycle ranges
f_z	Zero-upcrossing frequency of a signal
FC	Fuel consumption [ton]
$g(a)$	Stress intensity coefficient
g_c	Correction function for oblique wave
$\boldsymbol{G}$	Graph system for voyage optimization problems
H_s	Significant wave height [m]
H_σ	Transfer function of structural stresses
H_{dg}	Mean wave direction [deg]
J	Objective function
k	Slope parameter of the *S-N* curve for fatigue assessment
k_f	Frictional resistance correction factor
K	Stress intensity factor
m	Slope parameter in the Paris law for crack propagation analysis
N_0	Expected number of stress cycles
N	Number of cycles to failure
$\boldsymbol{N}$	Geographical waypoint
$\boldsymbol{p}$	Discrete power levels

$\boldsymbol{P}$	Ship state variable
P_b	Brake power [kW]
P_E	Effective power [kW]
R_A	Roughness allowance and still air resistance [N]
R_B	Resistance due to the bulbous bow [N]
R_F	Frictional resistance [N]
R_T	Calm water resistance [N]
R_W	Wave-making and wave-breaking resistance [N]
R_{AA}	Wind resistance [N]
R_{APP}	Additional resistance [N]
R_{AW}	Wave resistance [N]
R_{AWM}	Wave reflection resistance [N]
R_{AWR}	Ship motion-induced resistance [N]
R_{tot}	Ship total resistance [N]
S	Stress cycle range [MPa]
S_p	Stress perpendicular to the crack plane [MPa]
S_e	Encountered wave spectrum
S_w	Wave spectrum
S_x	Stress response spectrum under arbitrary sea states
SCF	Structural stress concentration factor
t	Time [h]
T_p	Peak wave period [s]
T_z	Zero-up-crossing (mean) wave period [s]
$\boldsymbol{U}(\boldsymbol{P})$	Ship control variable in the ship state $\boldsymbol{P}$
v_s	Ship service speed [m/s]
V	Ship speed through water [m/s]
V_g	Ship speed over ground [m/s]
V_u, V_v	Wind velocity towards east and north, respectively [m/s]
V_{WRref}	Relative wind velocity at the reference height [m/s]
w	Width of the crack plane [mm]
$\boldsymbol{w}$	A complete route/path-vector from the departure to the destination
$\boldsymbol{W}(\boldsymbol{P})$	Weather condition under the ship state $\boldsymbol{P}$
X	Structural stresses [MPa]

Greek letters

α	Intercept parameter of the *S-N* curve for fatigue assessment
ε	Spectral width parameter
η_0	Propeller open water efficiency
η_h	Hull efficiency
η_s	Engine shaft efficiency
θ	Ship heading angle [deg]
λ	Spectral moments
ρ_A	Mass density of air [kg/m^3]
σ_x	Standard deviation of X
Φ	Standard normal cumulative distribution function
Ψ_{WRref}	Relative wind direction at the reference height [deg]
ω	Wave frequencies [rad/s]

Abbreviations

ECMWF	European Centre for Medium-Range Weather Forecasts
ETA	Expected time of arrival
GHG	Greenhouse gases
IMO	The International Maritime Organization
LEFM	Linear Elastic Fracture Mechanics
MEPC	Marine Environment Protection Committee
RAOs	Response amplitude operators
RPM	Revolutions per minute
SEEMP	Ship Energy Efficiency Management Plan

1 Introduction

This chapter presents the research background for the thesis, followed by the motivations and objectives of the work. The outline, limitations and the delimitations of the thesis are presented.

1.1 Overall background

Shipping is recognized as the most efficient and cost-effective transportation mode, and carries approximately 90% of the world trade. It provides a dependable, low-cost means of transporting goods globally. It facilitates commerce and helps create prosperity among nations and peoples. However, ship emissions are a major source of air pollutants, e.g., sulfur dioxide (SO_2) and nitrogen oxides (NO_x). Because global shipping is recovering from the historic lows of 2016 (UNCTAD 2019), CO_2 and other greenhouse gas (GHG) emissions from the maritime sector have increased to comprise 3% of the global GHG emissions, emitting approximately 1 billion tons of GHG every year (Smith et al., 2015). Emissions from international shipping have directly and indirectly killed approximately 50,000 people a year in Europe, at an annual cost to society of more than €58 billion (Raaschou–Nielsen et al. 2011). All these factors have caused a major concern of environmental protection in the maritime community.

To protect the interests of the global environment and ecosystem, there have been many efforts to regulate air pollution from the shipping industry. The International Maritime Organization (IMO) established the Marine Environment Protection Committee (MEPC) to address environmental issues, including ship-source pollution such as oil, chemicals carried in bulk, sewage, garbage from ships and emissions, including air pollutants and GHG emissions. Table 1 lists several major activities in IMO addressing air emissions from international shipping.

Table 1. Major MEPC activities pertaining to international shipping air emissions.

Year	Event	Contents
1997	MARPOL Annex VI	Addressed ship air emissions and provided tools to reduce the adverse impacts from international shipping.
1998	MEPC 42	Began a program to monitor the average sulfur content of residual fuels from worldwide shipping.
2000	MEPC 45	An IMO study showed that the impact of ship nitrogen oxide (NOx) emissions continues to be the main policy driver.
2005	MEPC 53	Adopted amendments to the Regulations for the Prevention of Air Pollution from Ships in MARPOL Annex VI.
2008	MEPC 58	Approved the use of the Energy Efficiency Design Index (EEDI) method for new ships.
2009	MEPC 59	Disseminated measures to reduce GHG emissions from shipping.
2011	MEPC 62	Adopted revisions to MARPOL Annex VI and mandatory energy efficiency measures for international shipping.
2014	MEPC 67	Approved the Third IMO GHG Study and adopted mandatory measures to address the energy efficiency of international shipping.
2016	MEPC 70	Approved a roadmap for developing a comprehensive IMO strategy for reducing ship GHG emissions.
2018	MEPC 72	Adopted an initial strategy for reducing ship greenhouse gas emissions, setting a vision to reduce GHG emissions from international shipping.
2019	MEPC 74	Adopted amendments to MARPOL Annex VI, supporting consistent implementation of the 0.5% sulfur limit.

Table 1 also notes that ship energy efficiency is highly connected to air pollution and GHG emissions. In 1997, MARPOL Annex VI was adopted to limit air pollution from shipping. In

2011, IMO provided a suite of technical and operational measures, together with a ship energy efficiency framework, which were enforced starting in 2013. These mandatory measures further strengthened the energy efficiency requirements for the entire shipping industry. Many technical measures can be applied to increase a ship's energy efficiency. According to the shipping market survey conducted by DNV GL (2015), shipping companies have become more willing to invest in simple and cost-effective technical measures to reduce air emissions and fuel cost. Among all available energy-efficiency solutions, one of the most recognized measures is the voyage optimization, which more than 80% of the respondent shipping companies had planned to implement or had already installed in their ships.In addition, voyage optimization systems can help ships avoid encountering harsh sea environments leading to safer maritime transport. According to AGCS (2019), 46 ship losses occurred in 2018. Among all the causes of vessel loss, sunk/submerged is the most common, with 30 losses. The sunk/submerged losses were in large part due to encountering bad weather. Bad weather causes ship structural damage and cargo losses, or even loss of crew life. In recent decades, ship size has increased rapidly (OECD 2015). Larger vessels are more cost-effective and safer, while the cost of incidents has been increasing because of the cost of claims involving large vessels. Voyage optimization including weather monitoring and forecasting are widely used in ship navigation to avoid severe weather and enhance ship safety at sea.

Several commercial products of voyage optimizations are available in today's shipping market, including Storm Geo, WNI, GAC-SMHI Weather Solutions, etc. Storm Geo (2020) recommends optimal ship routes by analyzing variables, including weather, currents, speed, ship type and age, ship stability, and its cargoes. The models used in the system are established by artificial intelligence with an extensive alarm system that continuously monitors vessels and alerts the route analyst when action is needed. These alarms cover all facets of the voyage, including administrative details, data quality, ship energy performance, severe motion, etc. WNI (2020) offers a weather-routing service to provide safe and economical route and engine RPM options to achieve profits for operators, using ship-specific performance models. It gives options for voyage optimization, including least cost (time cost and fuel cost), required time of arrival (RTA) with least fuel, speed-based routing, etc. It also offers a multiple engine setting service for routing optimization. GAC-SMHI (2020) offers comprehensive weather solution services to ship operators to make their ship routing schedules. The system includes onboard weather routing tool and online performance analysis, which provide information of weather forecast and expected sailing time to make proper ship routing decisions.

For modern ship operations based on metocean forecasts, voyage optimization not only helps avoid bad weather but also finds routes that minimize transit time and fuel consumption without placing the vessel at risk of weather damage. Voyage optimization can provide an optimal route for voyages based on forecasted metocean data and a ship's individual characteristics for a transit (Bowditch 2002). With specified environmental condition constraints, an optimal route can refer to minimum fuel consumption, minimum traveling time, maximum safety, or a combination of these factors.

A typical voyage optimization system shown as in Fig. 1 consists mainly of the metocean data, the ship models, the constraints for sailing and operation, and the voyage optimization algorithms. The metocean data provides the potential sailing sea environments that a ship could encounter during the voyage. Various ship models are used to estimate a ship's operational performance when sailing at sea. These models are related to the objectives used in the voyage optimizations (including fuel consumption, expected time of arrival (ETA), crack propagation rate, fatigue damage, etc.). The constraints contain information about the traffic lanes, maximum continuous engine rating, etc. The core part of such a system is the voyage optimization algorithms, which generate optimal routes for different objectives based on

metocean forecasts, a ship's sailing constraints, individual characteristics, etc. Furthermore, a reliable voyage optimization system also requires accurate ship performance models. However, these performance models and metocean forecast data often contain uncertainties, which can largely affect the efficiency of voyage optimizations.

In addition to the direct impacts on a ship's operation by utilizing voyage optimizations, such as lower fuel consumption and air emissions, accurate expected time of arrival, etc., the voyage optimization systems may influence a ship's design conditions. For example, the long-term wave conditions encountered by voyage optimization aided ships may be significantly different from the original wave statistics from design guidelines. The difference can directly affect the fatigue and ultimate strength design of ship structures. Fatigue will be addressed in the thesis work, and other relevant researches are also briefly presented as follows.

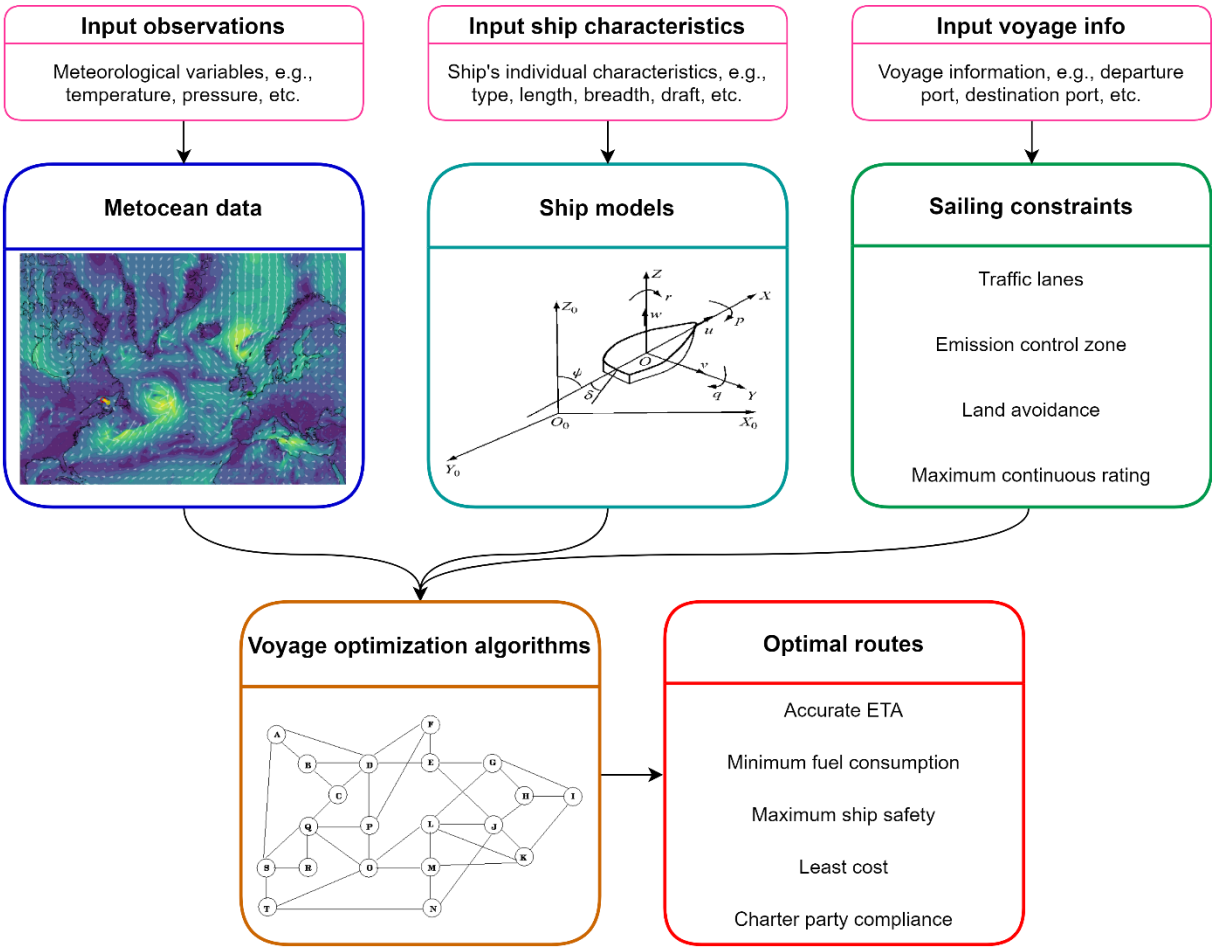

Fig. 1. Major components of a typical voyage optimization system.

1.2 Review on available voyage optimization algorithms

The review of conventional voyage optimization algorithms provides a foundation for understanding the pros and cons of current algorithms in the shipping market. According to the benchmark study of various existing optimization algorithms in **Paper A** (Wang et al. 2017), conventional algorithms often optimize a ship voyage with respect to a single objective, targeting either minimum fuel consumption or minimum ETA. Since total fuel consumption and required sailing time (related to ETA) along a voyage are often in conflict, optimizing one objective can result in sacrificing the other objective. Thus, single-objective optimization is

clearly insufficient for specific requirements. Additionally, conventional optimization algorithms operate under the assumption or constraint that ship speed or engine power output is fixed as a constant during the voyage. However, this may yield unrealistic optimal results because voluntary speed reductions are often needed when encountering harsh sea environments. Conventional voyage optimization algorithms normally refer to two-dimensional voyage optimization algorithms, including the modified isochrone method (Hagiwara, 1989), the isopone method (Klompstra et al. 1992), the dynamic programming method (Chen 1978; De Wit. 1990; Calvert 1990), Dijkstra's algorithm (Padhy et al. 2008), etc. These algorithms have been widely adopted in commercial software. Due to the limited accepted waiting time of shipping end-users to perform a voyage optimization (Larsson et al. 2015), conventional voyage optimization algorithms are the mainstream for commercial usage. They can provide optimal sailing course for a given voyage and can avoid or reduce the effects of specific adverse metocean conditions.

The isochrone method was first introduced by James (1957). An isochrone is defined as a geometrical time front, which is an achievable boundary for a ship during a certain time interval. Hagiwara (1989) modified the isochrone method to be more suitable for computer computation, contributing to its current wide use in the shipping market. The method can generate a ship optimal routing with minimum time cost under constant engine power. It can also be used to obtain a ship route with a minimum fuel cost by recursively adjusting the engine power for a minimum time-of-arrival route.

Klompstra (1992) introduced the isopone method, which is based on the modified isochrone method. It extends the isochrone method's search region into a three-dimensional sailing space by adding the time dimension into the geographic sailing regions. Its difference from the modified Isochrone method is that it creates energy fronts instead of time fronts. A fixed fuel unit is regarded as a grid resolution parameter in the isopone method. It is similar to a fixed time unit. Since it uses a deterministic relationship function between speed and fuel, it can also be regarded as a two-dimensional search method.

The dynamic programming method proposed by Bellsman (1952) is also widely used to solve voyage optimization problems concerning minimizing fuel consumption or accurate ETA. The method first predefines a grid system and then employs dynamic programming to search for the optimal solution at each stage of the voyage progress under constant engine power. The advantages of dynamic programming are two-fold. First, in a time-optimal route, once a waypoint is evaluated for the best time of arrival, the later waypoints in the grid system can also be evaluated without initiating a new dynamic-programming search. Second, this type of method can consider navigational constraints. In De Wit (1990), voyage optimizations using constant propeller revolution rate is proposed for both computationally and practically efficient optimization, since allowing for varying propeller revolution speeds in the optimization process could lead to serious computational difficulties.

Dijkstra's algorithm (Dijkstra 1959) has become a popular path-finding algorithm in the voyage optimization domain. Padhy et al. (2008) proposed utilizing Dijkstra's algorithm to solve the voyage optimization problem. The proposed method uses a grid formed by latitude and longitude lines, and the speed is based on a given engine setting. The weight functions for nodes and the routes are determined by considering both involuntary and voluntary speed reductions. The edges of the graph are weighted by transit time. Applying Dijkstra's algorithm to the defined graph yields the minimal time route.

More complex voyage optimization algorithms have been developed over the past decade to improve the capability and performance of voyage optimization. Those voyage optimization algorithms can be categorized into two major types: deterministic and stochastic algorithms.

1.2.1 Deterministic algorithms for voyage optimization

Deterministic algorithms are preferable for commercial use, as they can provide robust and concrete solutions. The dynamic programming method, Isochrone method, and Dijkstra's algorithm are considered the most suitable methods for voyage optimization problems (Wang et al. 2017). Table 2 lists the deterministic voyage optimization algorithms developed in the past decade. It includes their operational control variables and optimization objectives.

Table 2. Deterministic algorithms for voyage optimization.

Name of algorithms		**Operational control variable**				**Optimized objective**		
		Course	Speed	Power	RPM	Fuel	ETA	Others
3D dynamic programming	Shao & Zhou (2012)	✓	✓	×	×	↓	●	×
3D dynamic programming	Zaccone et al. (2017 & 2018)	✓	✓	×	×	↓	●	×
Dynamic programming	Skoglund et al. (2012)	✓	×	×	×	↓	↓	×
3D isochrone	Lin et al. (2013)	✓	✓	×	×	↓	↓	Distance
Improved isochrone	Roh (2013)	✓	×	×	×	↓	×	Distance
Dijkstra's algorithm	Veneti et al. (2017)	✓	×	×	×	↓	×	×
3D Dijkstra's algorithm	Wang et al. (2019)	✓	✓	×	×	↓	●	Fatigue damage
DIRECT method	Larsson et al. (2014)	✓	✓	×	×	↓	×	Weather impact

✓: involved; ×: not involved; Fixed: keep fixed; ↓ : minimum; ●: achieve required ETA;

The 3D dynamic programming method was introduced by Shao and Zhou (2012) for optimizing both a ship's sailing speeds and its headings along the voyage. It uses a float state technique to reduce iterations during optimization to reduce computational effort, and uses a discretized range of speeds in iterations to calculate the best speed-variation profile for the predefined objective function. During each iteration, one optimal state is chosen as the parent for the next state. Zaccone and Figari (2017) and Zaccone et al. (2018) rebuilt the 3D dynamic programming method model, attempting to select the optimal path and speed profile for a ship voyage based on metocean forecasts. Three variables are involved: starting and arrival waypoints and time instants. The search domain is progressively explored, following a breadth-first approach. Nodes are sorted by priority to minimize the estimated number of segments. A number of nodes characterized by a time of arrival and a cost are identified at the end of the calculation. The solutions given by each end waypoint form a Pareto-frontier for a two-objective optimization problem. Skoglund et al. (2012) proposed a new dynamic programming approach for multi-objective optimization by extending Dijkstra's algorithm. The method uses the concept of Pareto efficiency to handle multi-objective optimization, and can be used with both deterministic and ensemble weather forecasts.

Lin et al. (2013) proposed a 3D modified isochrone method for determining optimal ship routes. It utilizes the recursive-forward technique and a floating grid system. The recursive-forward algorithm for optimizing ship routing employs the weight (voyage progress) as a state variable. The advantage of the three-dimensional modified isochrone method is that it allows the ship speeds and ship headings to vary with geographic locations. In addition, it can not only minimize the ship's route and resistance but can also enhance the voyage safety in advance. Roh (2013) proposed an improved isochrone method for determining an economical ship route based on the acquisition of the sea state. The method is based on the original isochrone method (James, 1975). The author conducted a comparative study between the A* algorithm and the proposed method. A comparison was conducted among four objectives, i.e., computational performance, speed reduction, sailing distance and fuel consumption, and showed the improved isochrone method had better performance.

Veneti et al. (2017) presented an improved solution to the voyage optimization problem based on an exact time-dependent bi-objective shortest path algorithm that attempts to optimize two different conflicting objectives: fuel consumption and risk along the voyage. It creates a static square grid graph between the departure point and destination, with static information such as geographic and bathymetric information, and a dynamic grid that contains metocean conditions and updates itself when new data become available. Wang et al. (2019) proposed a scheme for applying Dijkstra's algorithm into a three-dimensional voyage optimization problem by predefining the voyage and the potential sailing time as a three-dimensional directed-weighted graph. The method can conduct multi-objective optimization, providing an accurate ETA and globally optimal solutions.

Larsson et al. (2014) introduced the DIRECT algorithm for ship voyage optimizations, which can find Great Circle routes, routing around obstacles such as islands, modifying speed to avoid a storm, and utilizing currents and wind to save fuel, based on the fuel consumption model from Maersk Maritime Technology. The advantage of this algorithm is that it provides fast convergence. However, the complexity of the optimization increases rapidly when the number of waypoints between the departure and the destination increases.

1.2.2 Stochastic algorithms for voyage optimization

It is more complicated for stochastic algorithms to establish appropriate models for solving voyage optimization problems, since the number of the variables is large and the variable dependencies are ambiguous. Table 3 lists the stochastic voyage optimization algorithms and their features.

Hinnenthal (2008) proposed a multi-objective genetic algorithm that stochastically solves a discretized nonlinear optimization problem. For computationally efficient optimization of the genetic algorithm, a ship's sailing course and velocity profiles are represented by parametric curves. This study's optimization objectives are two sets of parameters that control the parametric curves describing ship course and velocity. Marie and Courteille (2009) proposed another voyage optimization method based on a meshing procedure that defines a set of possible routes. The advantages of this meshing method are the physics-based definition of the rhombus and the low number of free variables used to define a route. Pareto-optimization with a multi-objective genetic algorithm (MOGA) is used for ship route optimization, providing a set of efficient solutions among different and conflicting objectives, under different constraints. Andersson (2015) introduced a method for multi-objective ship routing optimization, based on the distance-based Pareto genetic algorithm (DPGA) developed by Osyczka and Kundu (1995). The method can find a range of different Pareto optimal routes and conduct faster calculations than the grid search method.

Száapczynska et al. (2009) also proposed a multicriteria evolutionary weather-routing algorithm. The framework in the proposed algorithm is the normal genetic algorithm iterative process of population development, resulting in a Pareto-optimal set of solutions. The initialization of the objective to be optimized includes four routes: an orthodrome, a loxodrome, a time-optimized isochrone route, and a fuel-optimized isochrone route. Specialized operators are used for evolution, including a one-point crossover, a non-uniform mutation, and route smoothing by means of average weighting. Wang et al. (2018) proposed a hybrid voyage optimization algorithm based on a genetic algorithm and Dijkstra's algorithm. Dijkstra's algorithm is first implemented to obtain an optimal result; then, a genetic algorithm is applied to improve the results. The method can optimize a ship route with respect to multi-objectives and can provide optimal results with accurate ETA requirements.

Table 3. Stochastic algorithms for voyage optimization.

Name of algorithms		**Operational control variable**				**Optimized objective**		
		Course	Speed	Power	RPM	Fuel	ETA	Others
Multi-objective genetic algorithm	Hinnenthal (2008)	✓	✓	×	×	↓	↓	×
	Marie & Courteille (2009)	✓	Fixed	×	×	↓	↓	×
	Andersson (2015)	✓	✓	×	×	↓	↓	×
Genetic algorithm	Száapczynska et al. (2009)	✓	Fixed	×	×	↓	↓	×
	Wang et al. (2018)	✓	✓	×	×	↓	●	×
Real-coded genetic algorithm	Maki et al. (2011)	✓	✓	×	Fixed	↓	↓	Parametric rolling
	Wang et al. (2018)	✓	✓	×	×	↓	×	×
Strength Pareto evolutionary algorithm	Vettor & Soares (2016)	✓	✓	×	×	↓	↓	×
Non-dominated sorting genetic algorithm	Lee et al. (2018)	✓	✓	×	×	↓	↓	×
Ant colony algorithm	Tsou & Cheng (2013)	✓	Fixed	×	×	↓	●	×

✓: involved; ×: not involved; Fixed: keep fixed; ↓: minimum; ●: achieve required ETA;

Maki et al. (2011) introduced a real-code genetic algorithm technique searching for the optimum route. The optimization considers parametric rolling as one of its objective functions. The optimization results are robust and stable and can reduce the risk of parametric rolling. Wang et al. (2018) presented another version of a real-coded genetic algorithm to determine the minimum voyage route time for point-to-point problems in a dynamic environment. In this study, multi-population techniques and an elite retention strategy are employed to increase population diversity and accelerate convergence rates. The results show that the method can minimize voyage time and reduce the risk of encountering harsh weather conditions.

Vettor and Soares (2016) introduced a ship route optimization algorithm that uses the strength Pareto evolutionary algorithm to approximate the most favorable set of solutions for route optimization. The optimization objectives involve two sets of variables: one for the ship's position and the other for its speed. It uses Dijkstra's algorithm to generate the initial population, guaranteeing that all individual in the population is a feasible ship route solution.

Lee et al. (2018) proposed a method for simultaneously determining the path and the speed for routing problems. The method is based on the nondominated sorting genetic algorithm. A sensitivity analysis and a comparative study were conducted, which showed that the method can yield the route with the lowest fuel consumption compared with other methods.

Tsou et al. (2013) used the ant colony algorithm (Dorigo 1991) with a proper grid system to establish a route searching model that simulates a living organism's optimum behavior. By properly selecting the number of ants and the parameters, the algorithm's efficiency can be improved. The experimental results show that the method can help avoid heavy wind regions and reduce the risk of ship damage and cargo loss.

1.3 Uncertainties of metocean data and ship performance models

Voyage optimization algorithms, metocean forecast data, ship performance models, and navigation methods are considered as the most important input parameters for a voyage optimization method. Uncertainties in those input parameters can greatly influence the optimization results. According to the benchmark study on the performance of different voyage optimization algorithms (Wang 2018), using different algorithms can lead to different optimization results. Indeed, even for the same optimization algorithm, different parameter settings in the algorithm can result in different optimization results.

The accuracy of the metocean forecast data also greatly influences the quality of optimization results. Due to the complexity and imperfection of the physical description in today's metocean forecast models, as well as some uncertain and incomplete initial inputs into the forecast models, the metocean forecast data inevitably includes large uncertainties. The accuracy of metocean forecast is significantly reduced for time periods beyond 3-5 days. For example, the ensemble metocean forecast technique is used to provide information of the metocean forecast scatter. One ensemble forecast consists of 51 separate forecasts made by the same weather model, all activated from the same starting time. The starting conditions for each member of the ensemble are slightly different. Fig. 2 presents an example of significant wave height H_s (11th to 20th ensemble forecast data from the European Centre for Medium-Range Weather Forecasts (ECMWF)) for a waypoint located in the North Atlantic as in Fig. 2(a). It should be noted that the normal metocean forecast is one sample of the ensemble forecasts. The scatter of forecasted H_s widens after 3 days, indicating a decreasing metocean forecast accuracy.

Voyage planning includes four processes: appraisal, planning, execution and monitoring (IMO 1999; Bowditch 2002; Swift 1993). The appraisal process includes the collection of all information relevant to the voyage, i.e., the condition and state of the vessel, meteorological and oceanographic data, availability of services for voyage optimization, etc. Planning refers to plotting the intended voyage route, and designing a ship's route from berth to berth, preventing accidents by minimizing risk and navigating efficiently by reducing distance and fuel consumption. The execution and monitoring processes evaluate and monitor the ship operation to the plan and its compliance. During the planning process, the navigator determines the waypoints, the advance speed, and the expected time of arrival at each waypoint with the aid of voyage optimizations based on the data collected in the appraisal process (Bowditch 2002). If a voyage optimization algorithm is based on an uncertain metocean forecast, a generated

optimum ship route may contain large uncertainties. If the ship sails through the optimum route, her actual encountered sea environment may be worse than that without optimization.

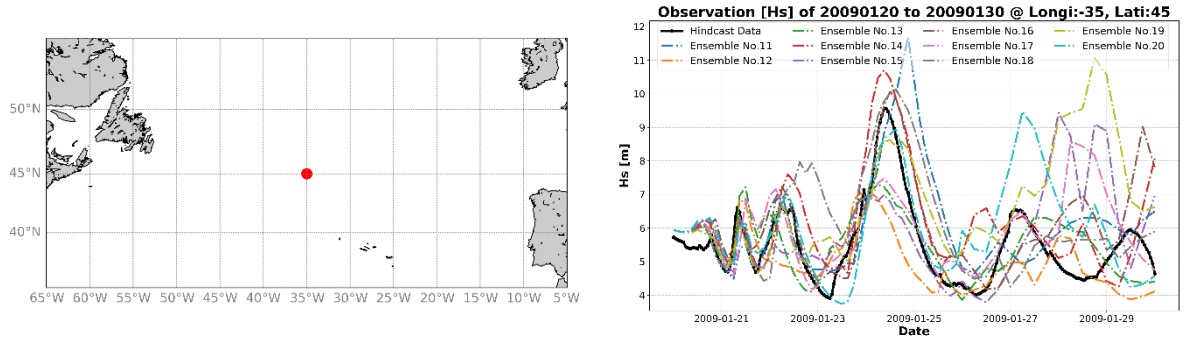

(a) (b)

Fig. 2. The investigation location at North Atlantic (a) and the comparison of significant wave height H_s for 10 ensemble metocean forecast samples and hindcast metocean data (b).

For example, according to a post-voyage analysis of a handy size container ship's winter navigation in 2008, the ship planned to sail significantly south of the Great Circle route to avoid harsh sea storms, based on the "uncertain" metocean forecasts (Mao et al. 2010). However, after the voyage, it was found that the ship encountered three storms along the "optimum" route, as shown in Fig. 3. If the ship was sailing along the traditional Great Circle route, the ship would have easily avoided the three storms. In the end, the result was a 100% increase in sailing time, a much higher fuel consumption, and risks associated with three large storms because the optimal route diverged from the Great Circle route.

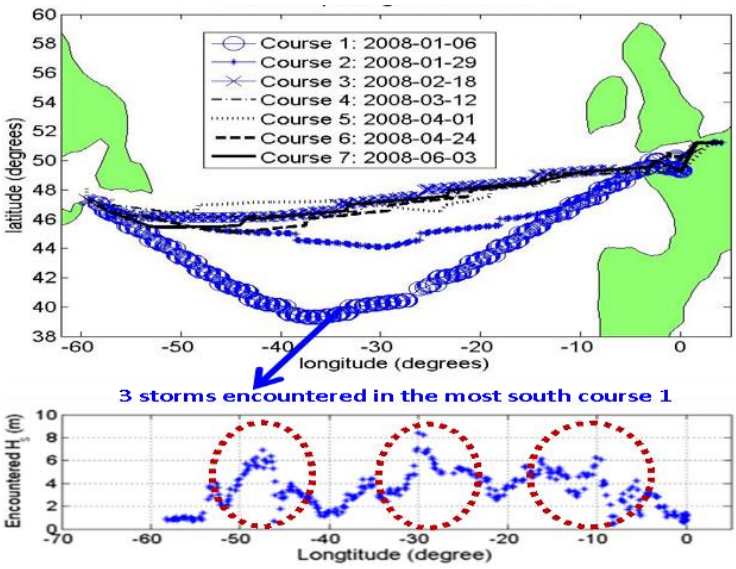

Fig. 3. A post-voyage analysis for a winter voyage (Course 1) that encountered three large storms when sailing along the optimum route generated based on uncertain metocean forecast.

Furthermore, the ship models used as objective functions estimating objectives, i.e., fuel consumption and ETA for voyage optimization algorithms, can also greatly affect the optimization results. For example, when the optimization target is minimizing ETA, the algorithms often attempt to set the ship's speed as high as possible. As a consequence, fuel consumption can be much higher than a voyage with a normal ETA. If the target is to minimize fuel consumption, a later ETA may result. For the same objective, different ship models can lead to different optimization results, as they could provide different objective values for the same ship state.

Additionally, different operational strategies are often used by captains to operate their ships, including sprint and loiter sailing (high-speed sailing for the majority of a ship's voyage, and slow speed in the final leg to ensure on-time arrival) (Ballou et al. 2008), constant speed, constant RPM or engine power sailing, etc. Furthermore, since a ship's resistance is normally proportional to her sailing speed to a power between 3 and 4, lowering a ship's sailing speed can significantly reduce her resistance and thus fuel consumption. Therefore, slow steaming is a common operation strategy today to minimize a ship's fuel consumption when sailing at sea. However, slow steaming can bring many challenges to shipping companies, such as the economic feasibility of longer sailing time for certain voyages. Furthermore, a ship's engine and propeller are designed with their highest propulsion efficiencies at a ship's service speed and RPMs. The engine and propeller running efficiencies of a slow steaming ship may be significantly reduced, leading to high total fuel cost. The reduced sailing speeds may also change the capability of a ship's voyage optimization strategy to avoid harsh sea environments.

1.4 Impact of voyage optimization application on ship fatigue

The main objective of most voyage optimization algorithms is to optimize a ship's voyage for fuel consumption and duration. However, ocean crossing ship structures are continuously subjected to various types of time-varying loads from the irregular sea waves, the propulsion system, and cargo operations, which may cause serious fatigue damage to ship structures. Since the encountered wave conditions are random, the accumulation of fatigue damage is also a continuous random process that should be considered during the ship design process. However, the uncertainties associated with numerical computations for wave loads, local structural stresses, description of local sea environments, and wave distributions, fatigue estimation models are difficult to consider during a ship's fatigue design stage.

For example, in Fricke et al. (2002), fatigue life analysis of a simple ship structural detail was benchmarked using different well-recognized ship design guidelines. The study showed that predictions for a ship's fatigue life using different methods/guidelines can differ greatly. Consequently, fatigue cracks may be initiated much earlier than a ship's actual design life. It may lead to the fact that fatigue cracks may widely exist in structural components of older ships, and they greatly challenge a ship's structural safety at sea.

Voyage optimization can be used to help ships sailing in calmer sea conditions. This was confirmed by Olsen et al. (2005) and Mao et al. (2010), who reported that real wave environments encountered by ships based on long-term full-scale measurements can differ significantly from those used in ship fatigue design. However, minimizing the rate of crack propagation or accumulation of fatigue damage in ship operations is usually not prioritized by the voyage optimization system. Thus, it is essential to investigate whether a ship fatigue routing which considers the crack propagation rate or the accumulation of fatigue damage as the optimization objective can further reduce the probability of encountering harsh metocean conditions and therefore mitigate the risk of structural failure.

During ship design, a calculation of the ship's wave-induced loads is indispensable. The calculation strongly depends on a reliable description of long-term wave environments encountered by the ship. Wave scatter diagrams are provided by the classification society guidelines as a joint probability distribution of significant wave height and mean wave period. They reflect the long-term distribution of waves encountered by ships sailing in specific areas. However, the effect of voyage optimization for ships on the encountered wave scatter diagrams has not been considered. Voyage optimization can be expected to reduce the probability of encountering heavy weather conditions and reduce the encountered wave-induced loads. Therefore, the actual wave environments encountered by ships that have installed voyage

optimization systems may not be consistent with that provided by the classification societies (Olsen et al. 2005; Mao 2010; Mao 2014).

1.5 Motivation and objective

Most of the complex voyage optimization algorithms concern speed optimization, since a ship's speed is one of the most crucial factors that influences its energy efficiency. According to IMO's energy consumption optimization study (IMO 2016), a speed reduction of 10% typically reduces fuel consumption per distance by approximately 20%. Optimizing the speed profile of a voyage can further improve the ship's energy efficiency during operation. However, existed voyage optimization algorithms concerning speed optimization can hardly provide global optimal solutions with accurate ETA for ship navigation, in addition to their lack of capability to conduct multi-objective voyage optimizations. Thus, it is indispensable to develop an optimization algorithm which can improve these algorithms.

Moreover, it is often difficult for shipmasters to control speed, especially for trans-ocean ships, since speed is greatly influenced by environmental conditions, which can easily lead to involuntary speed reduction. Indeed, for trans-ocean ships, engine power or propeller revolution is the dominant control parameter for shipmasters. Literature related to engine power optimization in voyage optimization problems is scarce because of the complicated relationship between engine power and ship speed. Thus, it is essential to develop a method capable of shaft power optimization which further eases the ship's operation while reducing operational cost.

In addition, the uncertainties from the input parameters/models for voyage optimization can greatly influence the optimization results. To assess the uncertainties from those input parameters/models, it is essential to conduct an uncertainty study to investigate the uncertainties of those variables. Finally, most of current voyage optimization algorithms aim to optimize a ship voyage for the objectives of fuel consumption and total sailing time (ETA). It is also important to investigate whether voyage optimization is applicable to other objectives such as fatigue damage, fatigue crack propagation during ship operations and ship design process.

The main objective of this thesis is to develop new voyage optimization algorithms and apply voyage optimization to ship's fatigue during operational period and design. The development of voyage optimization algorithms should address two areas: 1) improving commonly used voyage optimization algorithms; 2) investigating voyage optimization algorithm predictability with uncertain input parameters. Furthermore, today's voyage optimization is mostly focusing on improving energy efficiency (fuel saving) in ship operation. Investigations into its other potential applications, such as extending a ship's service life or ship design processes should be conducted. Five sub-tasks and research activities were carried out in this thesis to achieve these objectives:

1) To implement and compare commonly used voyage optimization algorithms and identify their basic characteristics, pros and cons for actual voyage optimizations.
2) To develop innovative voyage optimization algorithms that can overcome the limitations of conventional voyage optimization algorithms.
3) To propose a systematic approach to investigate how uncertainties of various input parameters can affect the results of voyage optimizations.
4) To investigate how the voyage optimizations can be used to mitigate the risk of ship structural failure du to large fatigue damage accumulation and crack propagation.
5) To study the impact of various ship voyage optimizations on a ship's long-term encountered wave environments and corresponding ship fatigue design.

1.6 Outline of the thesis

To achieve the overall objectives, research activities carried out in this thesis are summarized in the seven appended papers shown in Fig. 4. Voyage optimization algorithm development is conducted in **Papers A-D** and development of potential applications of voyage optimization algorithms is addressed in **Papers E-G**. In Chapter 2, the proposed methodology is described. It includes the description of general voyage optimization problems, the problem modeling defined in **Paper B** and **Paper C** and the algorithm implementation involved in the appended papers, except for **Paper F**. The cost functions, including the fuel consumption model, fatigue damage and fatigue crack propagation model used in the thesis are elaborated in Chapter 3. Selected important results and findings are presented in Chapter 4. The conclusions and contributions are presented in Chapter 5. Recommended future work is described in Chapter 6, and the references are listed in the end of the thesis.

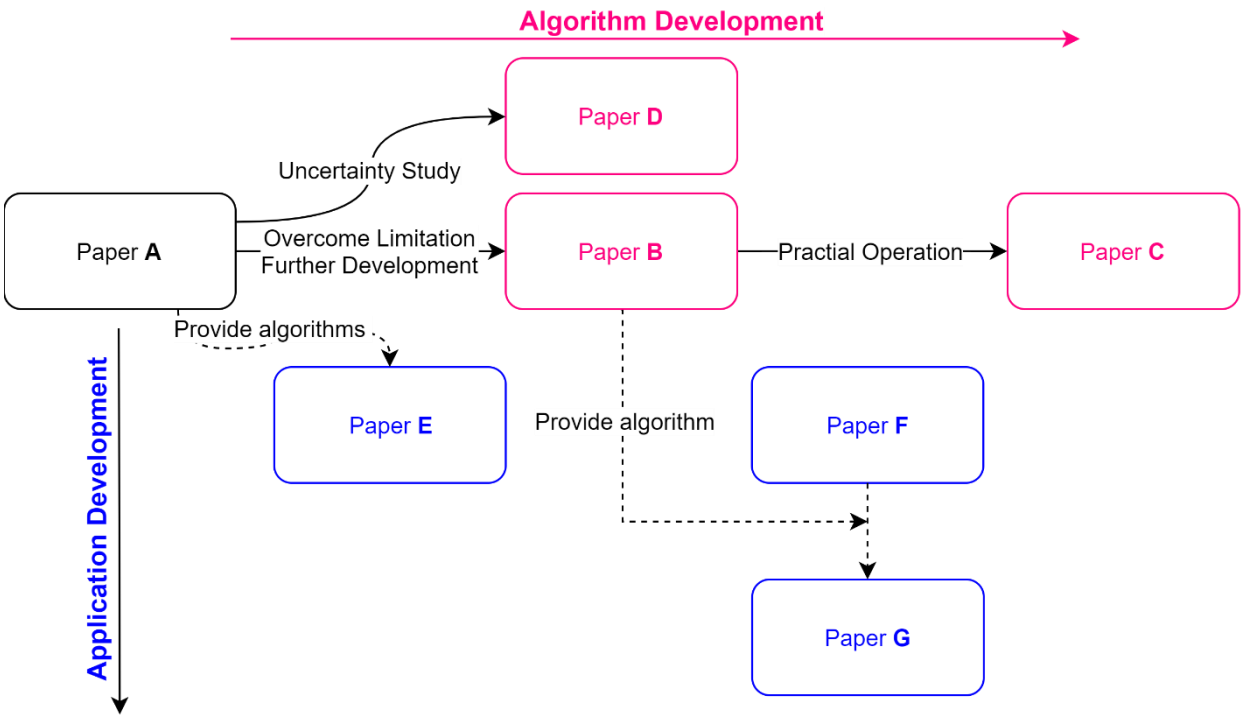

Fig. 4. Structure and workflow of the appended papers to achieve thesis objectives.

1.7 Limitations and delimitations

Many operational control variables are involved in a ship's operation, such as ship course, speed, engine power, etc. Course optimization is the most effective way to reduce the risk of encountering harsh sea conditions. Thus, it is adopted by most voyage optimization algorithms. The computability of such optimization algorithms is based on the discretization of the spatial region, which is the potential sailing area for ships. The calculations for the objectives such as fuel consumption, fatigue damage, and crack propagation are for the instantaneous state for a certain waypoint at a certain time. In this thesis, it is assumed that the instantaneous state is a mean state during a period of assumed stationary sea conditions. The total cost for an objective can be calculated through multiplying the mean state by the time duration.

Moreover, ship states such as the six degrees of freedom of ship motions and trim variations that cannot be accumulated over a long period of time (hours) are considered "ship transient states" and are not considered in this thesis. In the discrete form of the spatial region, the ship

state is usually calculated when the ship reaches certain waypoints. The metocean data which can be obtained at the waypoint with a specific time (the waypoint arrival time) is often a mean state of the metocean condition. Thus, when calculating the ship transient environment condition state, the mean state of the metocean condition does not reflect the actual ship state. During voyage optimization algorithm development, several assumptions must be made:

1) The hindcast data used as metocean inputs in the voyage optimizations is assumed to be the ground truth metocean environments encountered by the ships.
2) The metocean data used for the voyage optimizations are not updated during the optimization process.
3) The ship models are assumed to be accurate enough to reflect the ship real response and actual performance when sailing in specific sea environmental conditions.
4) Inputs of voyage optimization from the metocean data only contain the data of wind, waves and current. The influence of other environmental parameters, such as salinity, tide conditions, ice conditions, etc., on ship performance is assumed to be negligible.

Moreover, neither voyage optimization for arctic sailing nor plasticity-induced crack closure are considered in this thesis when the crack propagation is considered in the voyage optimizations. Material properties in the sea environment and corrosion are not considered in the fatigue assessment during the voyage optimization process.

2 Voyage optimization methodology

This chapter is divided into three subsections. In subsection 2.1, the mathematical description of general voyage optimization problems is presented. Section 2.2 introduces the formulation of specific voyage optimization problems defined in **Papers B** and **C**. In Section 2.3, representative algorithms implemented in this thesis for solving voyage optimization problems are briefly presented.

2.1 Mathematical description of voyage optimization problems

A ship's sailing route is defined as shown in Fig. 5 by a series of waypoints (forming the ship's trajectory) and their associated times of passing. A ship's state $\vec{\boldsymbol{P}}$ is defined by the waypoint and its associated arrival time.

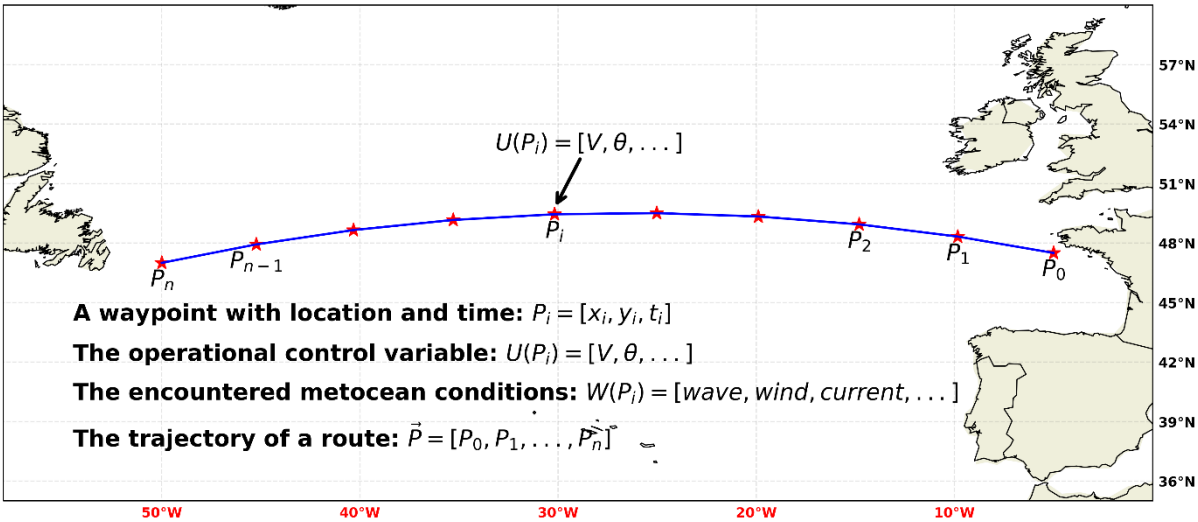

Fig. 5. An illustration of the ship route trajectory by its waypoints and operational conditions.

The ship's operational control variable $\boldsymbol{U}(\vec{\boldsymbol{P}})$ at ship state $\vec{\boldsymbol{P}}$ includes information such as the current velocity, heading, and engine power. For a simple description of general voyage optimization problems, the variables used to define a ship's sailing route are denoted as follows:

- Ship state variable: $\boldsymbol{P} = [x, y, t]^T$ where x, y, t represent longitude, latitude and time, respectively.
- Ship control variable: $\boldsymbol{U}(\boldsymbol{P}) = [V, \theta, \ldots]^T$, where V is the ship velocity and θ is its heading angle to form a ship's operational condition at one ship state $\boldsymbol{P}$. The ship control variable may contain other variables for ship operations such as engine power configuration and propeller revolutions.
- Metocean conditions: $\boldsymbol{W}(\boldsymbol{P}) = \left[H_s,\ T_z, H_{dg}, C_u, C_v, V_u, V_{v,\ldots}\right]^T$, representing the metocean conditions encountered during a ship state $\boldsymbol{P}$. H_s, T_p, H_{dg} represent the encountered wave conditions: significant wave height, mean wave period, wave direction, respectively. C_u, C_v represent the current velocities towards the east and north, and V_u, V_v are the wind velocities towards the north and east. The metocean conditions may contain other variables such as water salinity, tide conditions, etc., which are not considered in this thesis.
- Ship sailing constraints: $\boldsymbol{C}\left(\vec{\boldsymbol{P}}, \boldsymbol{U}(\vec{\boldsymbol{P}})\right)$, which include ship sailing constraints: geometric constraints and control constraints (land crossing constraints, marine engine power constraints, etc.). The function returns a Boolean value (true or false) that indicates the

feasibility of the sailing conditions under all the constraints. If true is received, the sailing condition of $\vec{\boldsymbol{P}}$ and $\boldsymbol{U}(\vec{\boldsymbol{P}})$ is validated and the ship can sail under the sailing condition.

For all ship states associated with the true value of the constraint function $\boldsymbol{C}\left(\vec{\boldsymbol{P}}, \boldsymbol{U}(\vec{\boldsymbol{P}})\right)$, the objective function J can be estimated by:

$$J = \int_{t_s}^{t_e} f_{ic}\left(\boldsymbol{U}(\vec{\boldsymbol{P}}), \boldsymbol{W}(\vec{\boldsymbol{P}})\right) dt \tag{1}$$

where $f_{ic}\left(\boldsymbol{U}(\vec{\boldsymbol{P}}), \boldsymbol{W}(\vec{\boldsymbol{P}})\right)$ is the instantaneous cost function for a ship state $\vec{\boldsymbol{P}}$ under control variable $\boldsymbol{U}(\vec{\boldsymbol{P}})$; t_s, t_e are the departure and arrival times, respectively. Here, the objective function for the voyage optimization problems can take different forms, e.g., fuel consumption, ship motions, expected time of arrival (ETA), fatigue damage accumulation, and crack propagation in a ship's structure (Wang et al. 2018).

The overall objective for optimum voyage planning is to find a series of suitable ship states $\vec{\boldsymbol{P}}$ and the associated operational control sets $\boldsymbol{U}(\vec{\boldsymbol{P}})$ that will lead to the minimum/maximum value of J due to optimum planning for the sea conditions $\boldsymbol{W}(\vec{\boldsymbol{P}})$ encountered at those waypoints. $\vec{\boldsymbol{P}}$ and $\boldsymbol{W}(\vec{\boldsymbol{P}})$ are the static variables used to describe states. A ship state $\vec{\boldsymbol{P}}$ and encountered metocean state $\boldsymbol{W}(\vec{\boldsymbol{P}})$ are determined by the operation control variable $\boldsymbol{U}$ from its previous state $\vec{\boldsymbol{P'}}$ and $\boldsymbol{W}(\vec{\boldsymbol{P'}})$. Thus, the target of the voyage optimization methods is to find an optimum operation control set $\boldsymbol{U}(\vec{\boldsymbol{P}})$ under a given initial state.

2.2 Voyage optimization modeling

Modeling is the art of formulating the application in terms of well-described problems. Proper modeling of voyage optimization problems is the key to applying algorithmic design techniques. Voyage optimization problems similar to routing problems on land can be modeled as path-finding problems. Modeling voyage optimization problems with path-find problems is the prerequisite for solving them; the essential matter is to create graphs that can properly reflect the problem. *"In graph theory, the shortest path problem is the problem of finding a path between two vertices (or nodes) in a graph such that the sum of the weights of its constituent edges is minimized"* (Kwon et al. 2007). Path-finding algorithms can be applied to solve the shortest path problem. Thus, by implementing a proper path-finding algorithm, the voyage optimization problems can be solved.

In this section, the modeling of two voyage optimization problems is presented: the **three-dimensional optimization problem** concerning the optimization of ship course and speed, and the **engine power optimization problem** concerning the optimization of ship course and engine power. In these two voyage optimization problems, the target is to find a ship operational control set $\boldsymbol{U}(\vec{\boldsymbol{P}})$ for a series of ship states $\vec{\boldsymbol{P}}$ to minimize fuel consumption and ETA. The difference is that in the three-dimensional voyage optimization problem, the ship operational control set $\boldsymbol{U}(\vec{\boldsymbol{P}})$ represents the ship's velocity and heading, and in the engine power optimization problem, $\boldsymbol{U}(\vec{\boldsymbol{P}})$ represents the engine power setting and the ship's heading.

2.2.1 Three-dimensional optimization modeling

The ship course optimization problem can be modeled by creating a two-dimensional graph system in the ship's potential sailing area. However, a two-dimensional graph is not adequate for solving the optimization problem involving both ship course and speed optimization. A

ship's speed depends on the sailing distance and associated travel time. Thus, the problem can be modeled by a graph with a spatial dimension and a temporal dimension.

In this thesis, the problem involving both ship course and speed optimization is modeled by a 3D graph system containing waypoints around a ship's potential sailing region and their associated arrival times. In this model, a voyage is discretized into stages to form a graph $\boldsymbol{G} = (\vec{\boldsymbol{P}}, \vec{\boldsymbol{A}})$, where $\vec{\boldsymbol{P}}$ is a set of predefined ship states containing the location and arrival time, and $\vec{\boldsymbol{A}}$ is a set of sub-paths/edges composed of state-pairs.

A simple example of the 3D graph is shown in Fig. 6. The 3D graph for a voyage denoted by $\boldsymbol{G} = (\vec{\boldsymbol{P}}, \vec{\boldsymbol{A}})$ can be generated by the following six steps:

1. Generate geographical waypoints (nodes) $\vec{\boldsymbol{N}}$ in the spatial region. The sub-paths/edges to connect waypoints between two adjacent stages are shown in the upper plot of Fig. 6. The voyage trajectory is divided into *n* stages along the reference course, which is taken here as the Great Circle. The distance of each stage between two adjacent waypoints along the reference route, $\Delta d_{gc} = v_s \cdot \Delta T$, where v_s is a ship's service speed, and the choice of ΔT depends on the temporal resolution of metocean forecast information, which is chosen as 3 hours here.
2. Generate an initial time set. A ship's speed is set to vary in the range $[0.5v_s, 1.2v_s]$. In the temporal region, the expected arrival time set for all waypoints in the *i*-th stage is denoted by:

$$\boldsymbol{\vartheta_i} = [t_{i,1}, t_{i,2}, \dots, t_{i,k}] = [\frac{\Delta T \cdot i}{1.2}, \frac{\Delta T \cdot i}{1.2} + \Delta t, \frac{\Delta T \cdot i}{1.2} + 2\Delta t, \dots, 2\Delta T \cdot i] \tag{2}$$

   where Δt is defined as the time interval of a sub-path for the *i*-th stage, and it is initialized based on the spatial resolution of the waypoints and the ship's input speed. All ship geographical states at the *i*-th stage, $\boldsymbol{N}_{i,j}$, j=1, 2, …, M, are assigned with the same passing/arrival time set $t_{i,k}$ (k =1, 2,..., K) to form an irregular multidimensional array $\boldsymbol{\vartheta}(i,j,k)$, shown by the red dots in the vertical direction of the lower plot in Fig. 6.
3. Since the number of potential arrival times at each stage, i.e., k, increases monotonically instead of exponentially as the stage advances, a feasible arrival time set for the *i*-th stage can be generated. The feasible time set is then assigned to each node $\boldsymbol{N}_{i,j}$ in the *i*-th stage. Then, the geographical waypoints $\boldsymbol{N}_{i,j}$ can be transformed into a ship state $\boldsymbol{P}_{i,j,k}$, shown as Eq. (3), where k represents the index referring to the feasible arrival time set $\boldsymbol{\vartheta}$. In Fig. 6 (lower plot), the red dots represent the accessible time set $\boldsymbol{\vartheta}$ for different stages and the black dots are eliminated from the initial time set [0, Δt, $2\Delta t$, …, $2\Delta T \cdot i$]:

$$\boldsymbol{P}_{i,j,k} = \boldsymbol{N_{i,j}}(t_{i,k}) = [x_{i,j}, y_{i,j}, \boldsymbol{\vartheta}(i,j,k)] \tag{3}$$

   $i = 1,2, \dots, N, j = 1, 2, \dots, M$, and k = 1,2,…,K that varies by stage.
4. Generate edge set $\vec{\boldsymbol{A}}$ for the graph. The edge generation of the nodes (ship states) from adjacent stages has certain constraints to mitigate the computation effort.
5. Calculate the cost (fuel consumption) for each individual edge. The edges contain the information for geographical location and passing/arrival times of both nodes, the distance between the nodes, and the ship's speed and heading. The metocean condition $\boldsymbol{W}(\boldsymbol{P})$ can be extracted based on the locations and times of the nodes. The metocean condition is chosen as encountered by the first node of an edge, and $\boldsymbol{U}(\vec{\boldsymbol{P}})$ is the ship's speed and

heading. The cost, as well as other outputs such as engine power and effective power for the ship sailing on this edge can be calculated.

6. Add the calculated data and extracted metocean data as attributes to the edges.

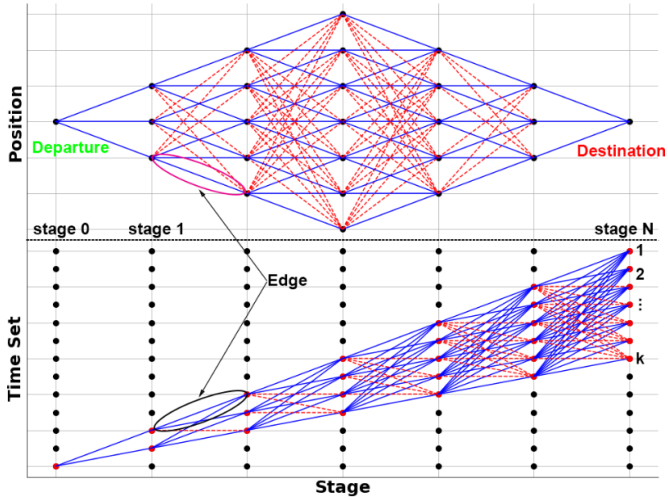

Fig. 6. An illustration of the 3D graph (a grid of waypoints) system.

A three-dimensional voyage optimization problem model concerning the optimization of ship course and speed is achieved by the above procedure. The output of this model is a three-dimensional weighted graph. An appropriate shortest path finding algorithm is required to find an optimal route on this graph.

2.2.2 Engine power optimization modeling

For ships sailing in rapidly changing environmental conditions in open sea areas, speed is difficult to control. Indeed, ships without strict restrictions on the voyage arrival time, such as tanker ships, are often controlled by engine power. In this problem model, two sets of variables are involved in this voyage optimization problem: the ship trajectory waypoints and the engine power configuration for the waypoints. The purpose of this model is to provide a scheme to compact two sets of variables of the ship operational control set $\boldsymbol{U}(\vec{\boldsymbol{P}})$ which can be properly used in the implemented genetic algorithm described in Section 2.3.2.

In this model, a grid/graph system $\boldsymbol{G} = (\boldsymbol{N}, \boldsymbol{A})$ is also generated. The graph is composed of a waypoint/node-set $\boldsymbol{N}$ and its corresponding sub-path/edge set $\boldsymbol{A}$ in the potential sailing area. An example of the grid/graph system deployed in the potential sailing area is shown in Fig. 7. The upper figure demonstrates the grid/graph system, and the lower figure shows its labeling system.

First, the potential sailing area is discretized into a series of stages (for example, M stages). The waypoints/nodes $\boldsymbol{N}$ in all the time stages and sub-paths/edges $\boldsymbol{A}$ connecting waypoints at adjacent time stages form a grid/graph system $\boldsymbol{G} = (\boldsymbol{N}, \boldsymbol{A})$. An example of the grid/graph system deployed is shown in Fig. 7. The upper plot demonstrates the grid/graph system and the bottom plot shows its corresponding labeling system. For example, the waypoint/node at the j_i-th state of the i-th stage of the grid system is denoted by $\boldsymbol{N}_{i,j_i}$, which contains geometric waypoint information, i.e., longitude $x_{i,j}$ and latitude $y_{i,j}$:

$$\boldsymbol{N}_{i,j_i} = (x_{i,j_i}, y_{i,j_i}) \tag{4}$$

The sub-path/edges $\boldsymbol{A}_{i,j_i}$ associated with waypoint $\boldsymbol{N}_{i,j_i}$ is formed by connecting it with all the waypoints in its preceding stage:

$$\boldsymbol{A}_{i,j_i} = \begin{bmatrix} \boldsymbol{A}_{i,j_i}(1) \\ \boldsymbol{A}_{i,j_i}(2) \\ \vdots \\ \boldsymbol{A}_{i,j_i}(k_{i-1}) \end{bmatrix} = \begin{bmatrix} (\boldsymbol{N}_{i-1,1} \rightarrow \boldsymbol{N}_{i,j_i}) \\ (\boldsymbol{N}_{i-1,2} \rightarrow \boldsymbol{N}_{i,j_i}) \\ \vdots \\ (\boldsymbol{N}_{i-1,k_{i-1}} \rightarrow \boldsymbol{N}_{i,j_i}) \end{bmatrix} \tag{5}$$

where k_{i-1} is the number of waypoints in the preceding (i-1)-th stage. A complete route/path vector $\boldsymbol{w}$ from the departure to the destination is formulated by selecting one adjacent sub-path/edge at each individual stage as:

$$\boldsymbol{w} = \left[\boldsymbol{A}_{2,j_2}(1), \boldsymbol{A}_{3,j_3}(j_2), \boldsymbol{A}_{4,j_4}(j_3), \dots, \boldsymbol{A}_{i,j_i}(j_{i-1}), , \dots, \boldsymbol{A}_M(j)\right] \tag{6}$$

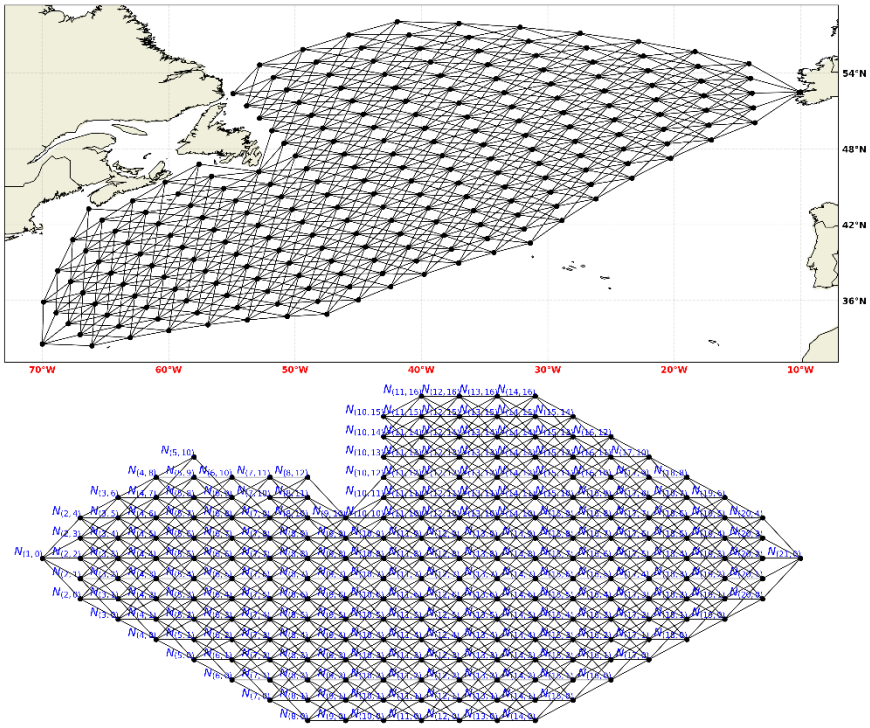

Fig. 7. A simple example of the grid/graph system and its labeling.

Second, a ship's engine power is configured such that only c discrete power levels $\boldsymbol{p}$ can be set for propulsion,

$$\boldsymbol{p} = [p_1, p_2, \dots, p_c] \tag{7}$$

Assigning one power level to each sub-path/edge of a path vector $\boldsymbol{w}$ can form a sample routing plan called a decision vector $\boldsymbol{D}$:

$$\boldsymbol{D} = \begin{bmatrix} \boldsymbol{w} \\ \boldsymbol{p}_f(\boldsymbol{w}) \end{bmatrix} = \begin{bmatrix} \boldsymbol{A}_{2,j_2}(1) \\ \boldsymbol{p}(\lambda_{2,j_2,1}) \end{bmatrix}, \begin{bmatrix} \boldsymbol{A}_{3,j_3}(j_2) \\ \boldsymbol{p}(\lambda_{3,j_3,j_2}) \end{bmatrix}, \begin{bmatrix} \boldsymbol{A}_{4,j_4}(j_3) \\ \boldsymbol{p}(\lambda_{4,j_4,j_3}) \end{bmatrix}, \dots, \begin{bmatrix} \boldsymbol{A}_{i,j_i}(j_{i-1}) \\ \boldsymbol{p}(\lambda_{i,j_i,j_{i-1}}) \end{bmatrix}, \dots, \begin{bmatrix} \boldsymbol{A}_M(j) \\ \boldsymbol{p}(\lambda_{M,j}) \end{bmatrix} \tag{8}$$

where $\boldsymbol{p}(\lambda_{i,j_i,j_{i-1}})$ is the power setting applied to sub-path $\boldsymbol{A}_{i,j_i}(j_{i-1})$.

The output of this model is a decision vector. In the genetic algorithm proposed in **Paper C**, the population composed of several decision vectors (which serve as candidate solutions) to the voyage optimization problem is evolved towards better solutions.

2.3 Algorithm implementation for problem solving

Dynamic programming, Dijkstra's algorithm, and the genetic algorithm are advertised by weather routing companies for solving voyage optimization problems (Chen 2013). In this thesis, they are categorized as deterministic and stochastic algorithms. The deterministic algorithms include dynamic programming and Dijkstra's algorithm, while the genetic algorithm is used as the stochastic algorithm in this thesis. In the following, the implementation of these algorithms is introduced.

2.3.1 Deterministic algorithm implementation

Dijkstra's algorithm (Dijkstra 1959) is implemented in the models of **Papers B** and **C** to solve specific voyage optimization problems. Dijkstra's algorithm is used mainly to find the shortest path with weighted graphs; the weight should be non-negative.

Comparing to the dynamic programming method, the main advantage is that Dijkstra's algorithm is well-structured and fit for weighted graphs. However, they would provide the same results when implemented in the same voyage optimization problem models defined in this thesis for the following reasons. First, the voyage in the model is divided stagewise, which means the ship cannot move further without crossing its next stage. Second, the graph is directed, which means the ship cannot move backward.

The following demonstrates the similarity and difference between the dynamic programming method and Dijkstra's algorithm implemented in the two-dimensional voyage optimization problem for ship course optimization.

Let $\boldsymbol{G}$ be a stagewise directed graph (as shown in Fig. 8) from the ship state $\boldsymbol{P}_1$ at its departure point via states $\boldsymbol{P}_{2,i_2}$, $\boldsymbol{P}_{3,i_3}$ ..., $\boldsymbol{P}_{m-1,i_{m-1}}$ to the state $\boldsymbol{P}_m$ at the destination point. Fig. 8 shows an example of the approaches for finding optimal sub-paths from ship state $\boldsymbol{P}_1$ to $\boldsymbol{P}_{3,3}$ using dynamic programming and Dijkstra's algorithm.

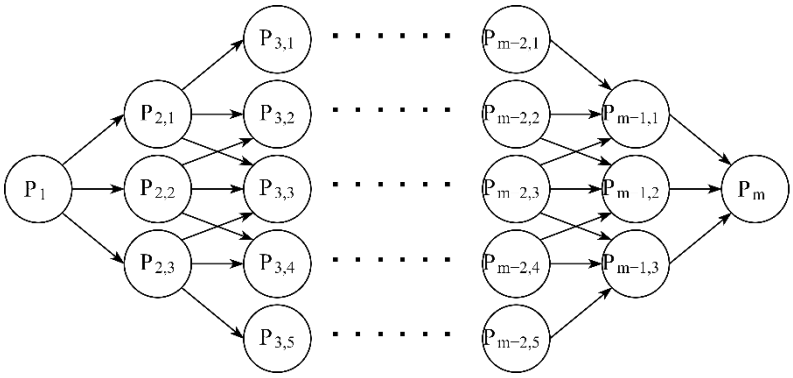

Fig. 8. A stagewise directed weighted graph.

Dynamic programming is implemented with a back-forward approach for computational efficiency. Fig. 9 (a) shows an example of finding the minimum-cost sub-path for $\boldsymbol{P}_{3,3}$ using dynamic programming.

1) Find all the states which can reach $\boldsymbol{P}_{3,3}$ from a back/previous stage.
2) For all sub-paths which can reach $\boldsymbol{P}_{3,3}$, find the minimum-cost sub-path, which is $\boldsymbol{P}_1 \rightarrow \boldsymbol{P}_{2,2} \rightarrow \boldsymbol{P}_{3,3}$.
3) Following the same approach, the optimal minimum cost sub-paths for all other states in the same *i*-th (current 3rd) stage as $\boldsymbol{P}_{i,j}$ can be found. Subsequently, the minimum-cost sub-path from $\boldsymbol{P}_1$ to $\boldsymbol{P}_{i,j}$ is stored.
4) Search forward by repeating this procedure until the destination point is reached; the result yields the minimum-cost optimal ship route in the graph.

Dijkstra's algorithm is implemented with a priority queue structure to store the sub-paths and their associated costs. In a priority queue, an element with a lower cost will be used before an element with a higher cost. Fig. 9 (b) shows an example of finding the minimum-cost sub-path for $\boldsymbol{P}_{3,3}$ by Dijkstra's algorithm.

1) The state $\boldsymbol{P}_{2,1}$ first visits $\boldsymbol{P}_{3,3}$. The queue stores $\boldsymbol{P}_{3,3}$ with the sub-path and its cost for $\boldsymbol{P}_{2,1} \rightarrow \boldsymbol{P}_{3,3}$.
2) $\boldsymbol{P}_{2,2}$ then visits $\boldsymbol{P}_{3,3}$ with a lower-cost sub-path, and the queue replaces the previous sub-path $\boldsymbol{P}_{2,1} \rightarrow \boldsymbol{P}_{3,3}$ with $\boldsymbol{P}_{2,2} \rightarrow \boldsymbol{P}_{3,3}$.
3) Finally, $\boldsymbol{P}_{2,3}$ visits $\boldsymbol{P}_{3,3}$ with a higher-cost sub-path. The program will do nothing.
4) Repeat this procedure until the last state (destination) is visited; the result yields the optimal route.

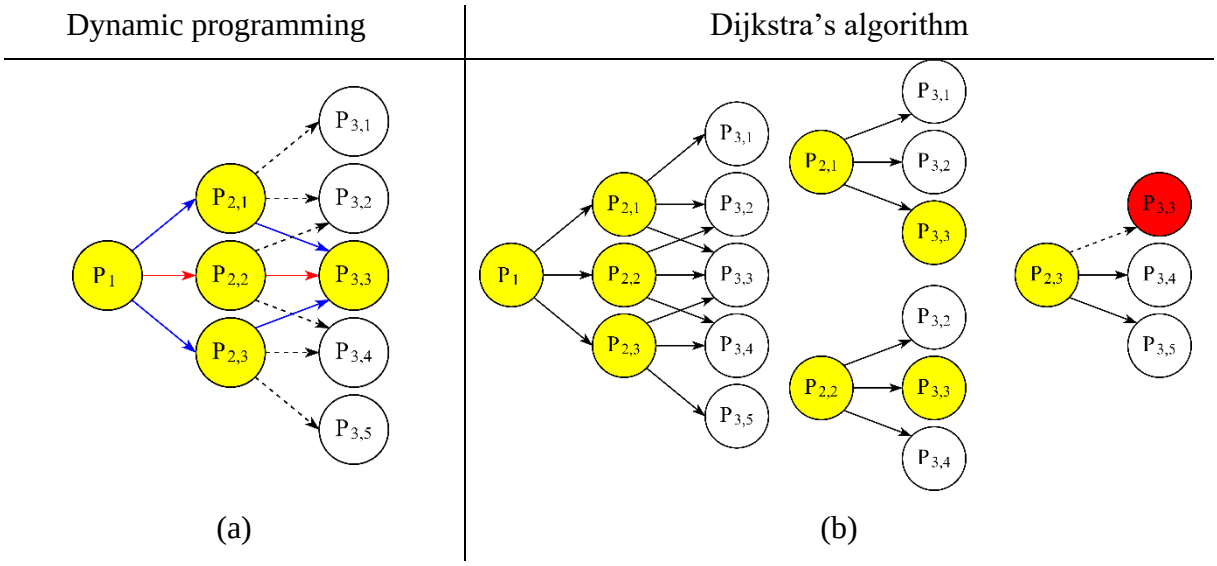

Fig. 9. Difference in finding optimal sub-paths between dynamic programming (a) and Dijkstra's algorithm (b).

The implementation of dynamic programming for voyage optimization problems is flexible. In addition to a back-forward approach, it can also be implemented in the same way as Dijkstra's algorithm. Dijkstra's algorithm has a fixed pattern of implementation for solving shortest-path problems. Since the graph for the voyage optimization problems modeled in this thesis is stagewise and directed, the optimization results from dynamic programming and Dijkstra's algorithm for the same problem should be identical.

2.3.2 Stochastic algorithm implementation

Stochastic algorithms, such as genetic algorithms and ant-colony algorithms, are widely used for solving voyage optimization problems (Hinnenthal 2008; Marie and Courteille 2009; Záapczynska et al. 2009; Maki et al. 2011; Tsou et al. 2013; Andersson, 2015; Vettor & Soares

2016; Lee et al. 2018; Wang et al. 2018). They can provide globally optimal solutions and execute multi-objective optimization for voyage optimization problems. Such algorithms begin with a set of feasible solutions, and then improve them by evolving the ship's operational control variables, such as ship course, speed and engine power. The algorithm is never assured to reach the optimum (Chen 2013). The shortcomings of stochastic algorithms in this voyage optimization problem are quite noticeable. The initialization of stochastic algorithms such as the genetic algorithm, the particle swarm algorithm and the ant colony algorithm can highly influence the convergence of the optimization and the robustness of the optimization results. Additionally, the samples that must be evolved in voyage optimization problems usually contain many variables. Without proper sample size and selection, the result may converge to a locally optimal point, or even be unable to find a proper solution.

In **Paper C**, the engine power-based optimization problem is solved by the genetic algorithm combined with deterministic algorithms that can overcome the shortcomings of the genetic algorithm in voyage optimization problems. Since a decision vector contains many variables, it is difficult to directly apply the genetic algorithm to this complex problem. Deterministic algorithms can generate locally optimal solutions by fixing several variables. For example, Dijkstra's algorithm is used to find the path vector optimal solutions by fixing the engine power configuration vector. The optimal solutions for the engine power configuration vector are obtained by using dynamic programming with fixed path vectors. Those solutions can guide the genetic algorithm evolution in the right direction for fast convergence. The workflow is depicted in Fig. 10, and its implementation involves the following 6 steps:

1) Generation of the initial population by deterministic methods (Dijkstra's algorithm and Dynamic programming method). The individual samples in the population represent the decision vector described in Sub-section 2.2.2.
2) Calculation of the fitness values of each decision vector of the population. Each decision vector contains two design variables, i.e. fuel consumption and sailing time.
3) Selection of candidate solutions (routes). Since two design variables are involved in the optimization, multi-objective optimization is used in the population selection step. Instead of ranking the members with their fitness values for the selection, Pareto optimal solutions are selected as part of the candidates for the next generation.
4) Evolution of the population. The crossover operator is used to combine the genetic information of two parents to generate new offspring, and the transfusion operator uses a deterministic method and a stochastic method to generate new offspring to increase the population diversity.
5) Termination of the optimization. The maximum iteration number is adopted as the termination criterion. If the iteration number reaches the termination criterion, the optimization will stop.
6) Find the optimal solution (route). The optimal solution is found in the Pareto front of the last generated population based on the overall objectives from ship operators.

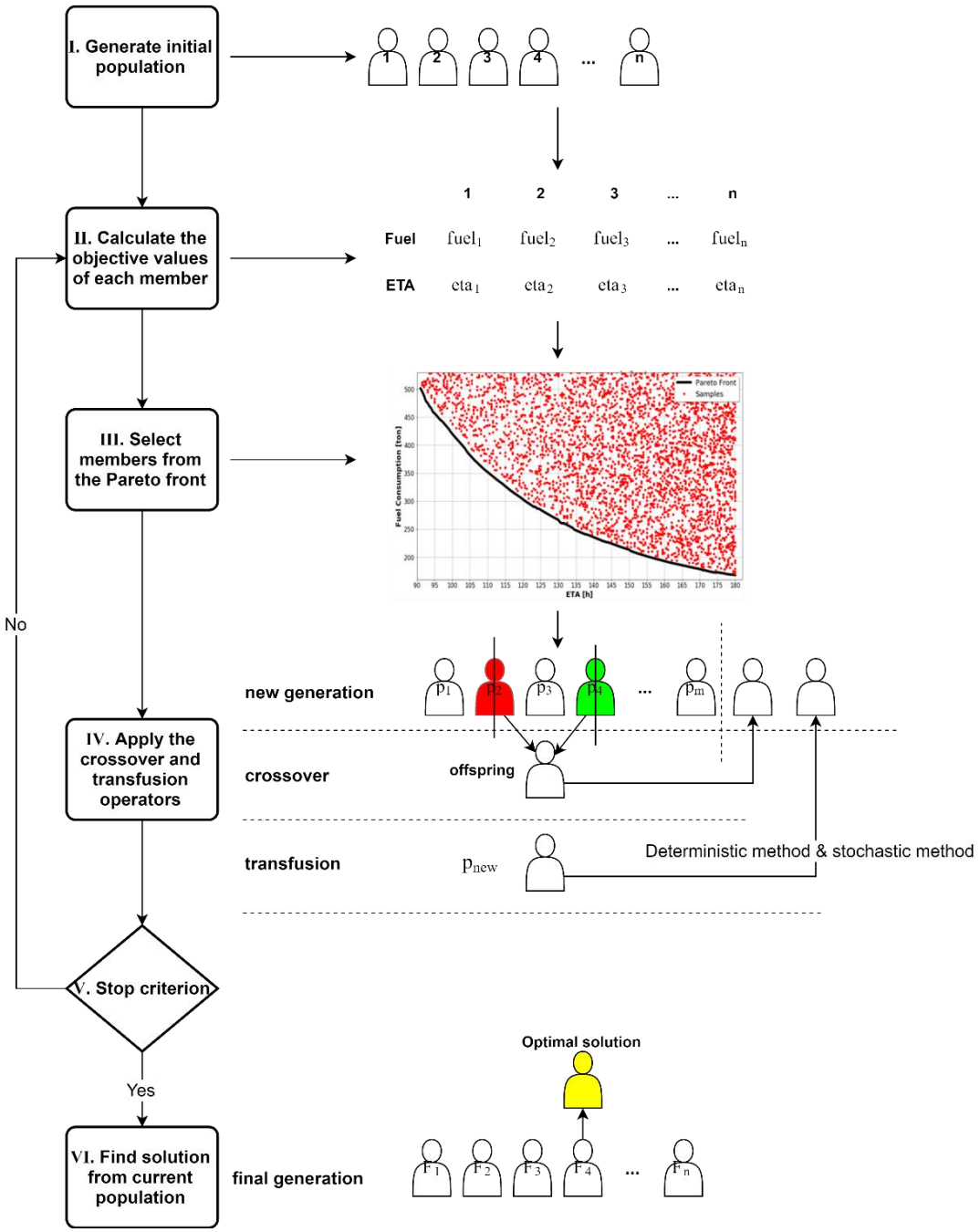

Fig. 10. The workflow of implemented genetic algorithm in the thesis.

3 Cost functions in voyage optimization algorithms

This chapter describes the cost functions applied in the voyage optimization algorithms. The cost functions are represented by different ship performance models, i.e., the fuel consumption model, the fatigue crack propagation model and the fatigue damage model. The models are used to calculate the cost under various environmental conditions.

The models describe a ship's performance, e.g., sailing speed (Kwon 2008), motion/damage response (Mao 2014), and fuel cost (Tillig et al. 2017), in terms of its loading conditions, encountered weather conditions, and operational conditions. These models are the core elements in a voyage optimization process to estimate the cost function for specific objectives. The fuel consumption model describes a ship's speed and fuel consumption relationship as a function of the ship's main dimensions, status and sea conditions. The fatigue damage accumulation model and fatigue crack propagation model are used to predict the fatigue damage accumulation rate and the crack propagation rate in the ship structures based on ship characteristics, ship status and encountered metocean conditions.

3.1 Fuel consumption estimation model

The energy-transfer system in a ship is complex process (Tillig et al. 2017) and contains many components, such as the ship resistance, hull efficiency, relative rotative efficiency, etc. To describe a ship's speed-fuel relationship, the most important component is to accurately estimate a ship's resistance in different conditions (Kwon 2008). Ship resistance can be divided into three parts, calm water resistance, added resistance due to waves and added resistance due to wind. Calm water resistance is one of the most important parts in describing a ship's resistance. Its proportion to the total resistance will eventually determine the choice of ship route by the voyage optimization algorithm chosen. Since metocean conditions are the main factors in voyage optimization problems (Bowditch 2002), an accurate model for estimating the added resistance due to waves is thus an important input for a voyage optimization system. When sailing in severe sea conditions, added resistance due to waves will lead to a significant reduction of ship speed. Finally, added resistance due to wind is relatively small but crucial due to the direction of the wind for determining the heading angle in a voyage.

The workflow for the ship speed-fuel prediction used in this thesis is presented in Fig. 11. It is a typical estimation procedure to predict the fuel consumption rate using input parameters of encountered metocean conditions, the ship's individual characteristics, operational profiles, etc. This procedure has been implemented into an in-house code using the following mathematical formulas.

Mathematically, for a sailing state at the waypoint $\boldsymbol{P}_i$ of $\boldsymbol{U}(\boldsymbol{P}_i)$ in a stationary sea state $\boldsymbol{W}(\boldsymbol{P}_i)$, (lasting from 20 minutes to 6 hours), a ship's fuel consumption during the period of the stationary metocean condition can be estimated by:

$$FC = P_b \cdot c_{sfoc} \cdot (t_{i+1} - t_i), \quad P_b = \frac{R_{tot} \cdot v_g}{\eta_0 \cdot \eta_h \cdot \eta_s} \tag{9}$$

where v_g is the ship speed and R_{tot} is the total ship resistance in the state, c_{sfoc} is the specific fuel oil consumption (unit: g/KWh), t_{i+1} - t_i is the sailing time from the i-th stage to the next stage and it varies depending on individual nodes/waypoints, η_h, η_0, η_s are the hull efficiency, propeller open water efficiency, and engine shaft efficiency, respectively. The three efficiencies η_h, η_0, η_s are obtained from the propeller-engine diagram and the specific fuel oil consumption c_{sfoc} is retrieved from the engine SFOC diagram based on the shaft power P_b.

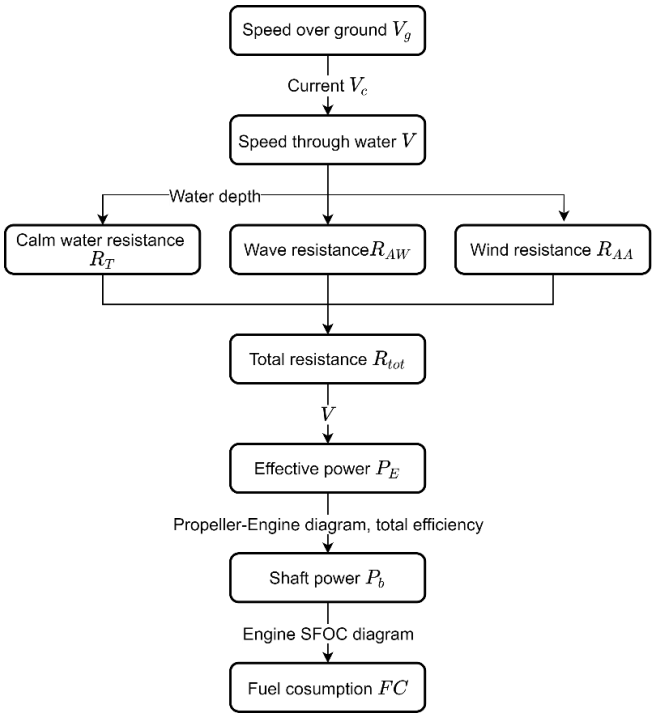

Fig. 11. Ship speed-fuel prediction flowchart for routing optimization.

As shown in Fig.11, the estimation of the total resistance R_{tot} is one of the most important procedures for estimating fuel consumption. The total resistance R_{tot} is regarded as a function of ship operational condition $\boldsymbol{U}$ and metocean condition $\boldsymbol{W}$ at the sailing waypoint in voyage optimization process, i.e., $R_{tot} = f\big(\boldsymbol{U}(\boldsymbol{P_i}), \boldsymbol{W}(\boldsymbol{P_i})\big)$. It is estimated based on the speed through water V, which is calculated from the speed over ground on V_g by considering the effect of the ocean current velocity. To estimate the ship's total resistance R_{tot}, it can be decomposed in accordance with the following equation:

$$R_{tot} = R_T + R_{AA} + R_{AW} \tag{10}$$

where R_T is the calm water resistance, $R_{AA}$is the wind resistance, R_{AW} is the added resistance due to waves.

Calm water resistance

The calm water resistance R_T can be estimated by the Holtrop-Mennen (1983) method viz:

$$R_T = \big(1 + k_f\big)R_F + R_W + R_{APP} + R_A + R_B \tag{11}$$

where:

k_f	Frictional resistance correction factor.
R_F	Frictional resistance.
R_W	Wave-making and wave-breaking resistance.
R_{APP}	Additional resistance.
R_A	Roughness allowance and still air resistance.
R_B	Resistance due to the bulbous bow.

In the Holtrop-Mennen method, the above items are computed by empirical formulas in terms of, e.g., a ship's main dimensions, ship type, the dimensions of the bulbous bow and immersed transom, etc. Those formulas are derived based on a large number of model tests and can give a rough estimate of a ship's calm water resistance.

Added resistance due to wind

The resistance increase due to wind can be calculated according to ISO 15016:2015(E) by the formula below:

$$R_{AA} = 0.5\rho_A \cdot C_{AA}(\Psi_{WRref}) \cdot A_{XV} \cdot V_{WRref}^2 - 0.5\rho_A \cdot C_{AA}(0) \cdot A_{XV} \cdot v_g^2 \tag{12}$$

where:

R_{AA}	is the resistance increase due to relative wind.
A_{XV}	is the transverse projected area above the waterline including superstructures.
C_{AA}	is the wind resistance coefficient; $C_{AA}(0)$ means the wind resistance coefficient in head wind.
v_g	is the measured ship's speed over ground.
V_{WRref}	is the relative wind velocity at the reference height.
Ψ_{WRref}	is the relative wind direction at the reference height.
ρ_A	is the mass density of air.

Added resistance due to waves

The added resistance in waves can significantly affect a ship's total fuel consumption for an ocean crossing voyage. To estimate such resistance in actual sea state, added resistance due to regular waves of a unit wave amplitude and a series of wave frequencies ω at an operational profile [V, θ] is often divided into two components:

$$R_{AW}(\omega|V,\theta) = (R_{AWR}(\omega|V) + R_{AWM}(\omega|V)) \cdot g_c(\theta) \tag{13}$$

where R_{AWR} and R_{AWM} denote wave reflection and ship motion-induced resistances, V and θ represent a ship's speed and heading angle. Different empirical formulas and hydrodynamic theory-based numerical methods are available to get the added resistance due to waves. In this thesis, the semi-theoretical formulas proposed by Liu and Papanikolaou (2016) are used to estimate the Response Amplitude Operators (RAOs) of R_{AWR} and R_{AWM} but only for head sea operations.

Inspired by the ideas from Alexandersson (2009), a correction function $g_c(\theta)$ is used to model the impact of heading angles for added resistance in waves. The correction function is established for specific ships based on their measurement data. Then the mean added resistance due to an actual sea state (of irregular waves represented by a significant wave height H_s and mean wave period T_z) described by an ITTC wave spectrum $S_w(H_s, T_z)$, can be computed by:

$$R_{AW}(H_s,T_z,V,\theta) = \int_0^{+\infty} S_w(H_s,T_z) R_{AW}(\omega|V,\theta) d\omega \tag{14}$$

In addition, other added resistances due to shallow water effect, water temperature are simply estimated by the method proposed in ISO15016 (2015).

This fuel consumption estimation model in Fig. 11 is implemented in **Paper A-E** and **G**, and has been validated in **Paper B-D** such that it can be used to predict the relationship between ship speed and fuel consumption rate under various metocean conditions.

3.2 Fatigue damage accumulation model

Ship structures are designed to behave elastically during its design life of around 20 years. The fatigue strength is assessed by stress-based approaches, i.e. high-cycle fatigue design principles. In the analysis, the material behavior is characterized by an *S-N* curve, with a log-linear dependence between the number of cycles to failure *N*, and the stress cycle range *S*, $\log(N) = \alpha - k\log(S)$. Different *S-N* curves exist for different materials, geometries, welds, etc., the parameters α and k are usually categorized based on the properties of structural details in the class rules. The stress ranges, here denoted by S_i, ($i = 1,\ldots,n$), can be obtained by the rainflow counting method for each sea state. Finally, the accumulated damage is calculated using the linear Palmgren-Miner law as:

$$D(T) = \sum_{i=1}^{n} \frac{S_i^k}{\alpha} \tag{15}$$

In addition to the rainflow counting method, Fig. 12 shows a schematic of a procedure for the direct calculation of structural stresses. It is essential for a reliable fatigue analysis that reliable encountered wave environments are used in the calculation, i.e. the long-term distribution of sea states. In class rules, it is given as the wave scatter diagram, which can present an overall distribution of waves for all ships sailing in the same region. However, this diagram can rarely consider the practical operation conditions for an individual ship. More and more ships are equipped with weather routing systems, which can help the ships to avoid large storms. As a positive result from a fatigue damage accumulation point of view, the real encountered wave environments may differ significantly from the wave scatter diagram which is used in the design.

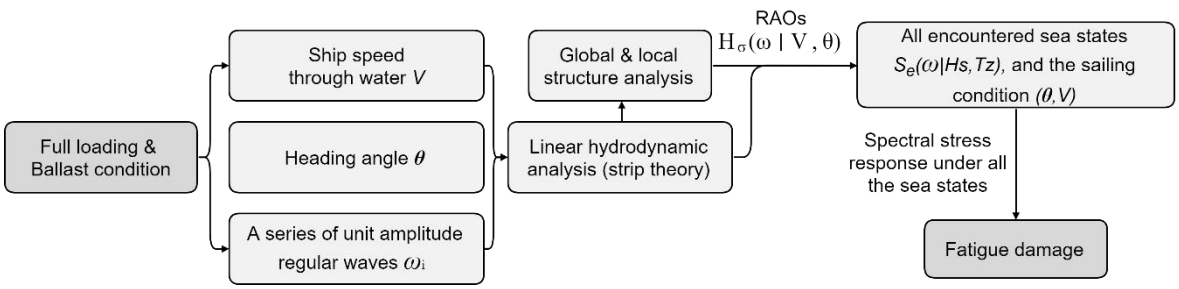

Fig. 12. Example of the workflow of a conventional ship fatigue life prediction method with fatigue loads from direct calculations.

For ship structural fatigue analysis, ship stress response along a ship route, i.e., $\vec{\boldsymbol{P}}$ and $\boldsymbol{U}(\vec{\boldsymbol{P}})$ here**,** is often divided into a series of stationary periods of metocean information, $\boldsymbol{W}(\vec{\boldsymbol{P}}) = \boldsymbol{W}_1$, $\boldsymbol{W}_2$, …, $\boldsymbol{W}_n$. A sea state $\boldsymbol{W}$ is described by a classical wave spectrum $S_W(\omega)$, e.g., Pierson-Moskowitz, JONSWAP, etc., which is a function of significant wave height H_s and wave period T_z shown in Fig. 13 (a). The transfer function or response amplitude operators (RAOs) of structural stresses is obtained for various ship speeds and heading angles $\boldsymbol{U} = [V, \theta]^T$. It is denoted by $H_\sigma(\omega|V, \theta)$ shown in Fig. 13(b).

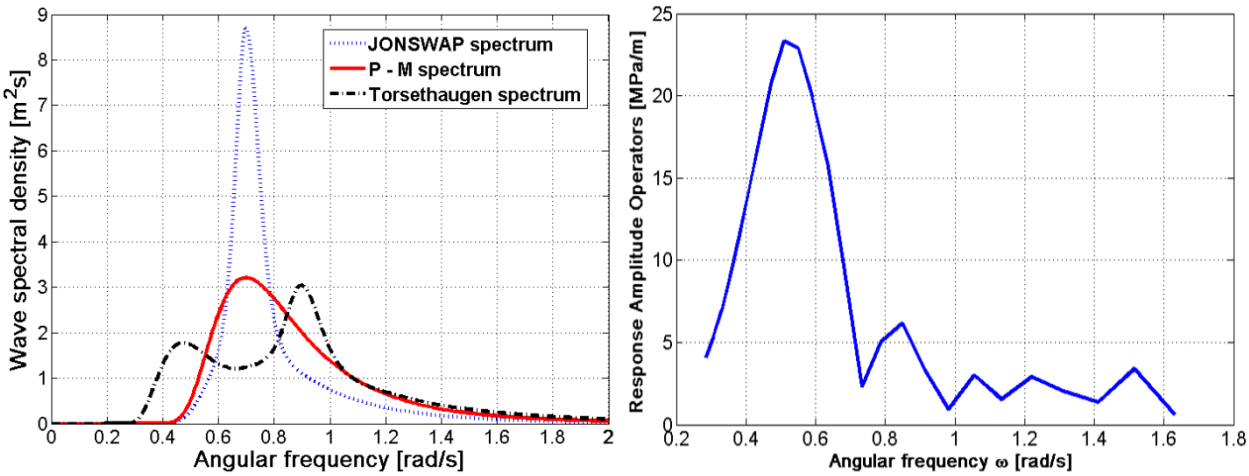

(a) (b)

Fig. 13. Three typical wave spectra stress (a) and RAOs of a deck longitudinal stiffener (b).

The variability of structural stresses, denoted by $X(t)$ here, is mainly caused by the change of the wave loadings applied on ships. Hence, it is essential to get the correct wave (hydrodynamic) loads. The structural stresses due to the wave loads can be computed by beam theory. The stress is often assumed to be Gaussian and is uniquely defined by its mean value and spectrum. For a specific sailing speed V and heading angle θ, the stress response spectrum under arbitrary sea states can be computed by:

$$S_x(\omega|V,\theta,H_s,T_z) = |H_\sigma(\omega|V,\theta)|^2 S_e(\omega|H_s,T_z)d\omega \tag{16}$$

where $S_e(\omega|H_s,T_z)$ is the encountered wave spectrum that cannot always be explicitly expressed for all wave frequencies. Instead, it is enough to only obtain the spectral moments of the ship response for a ship's structural integrity assessment. The n-th order spectral moments can be calculated by:

$$\lambda_n = \int_0^\infty \left|\omega + \frac{\omega^2 V\cos\theta}{g}\right|^n H_\sigma^2(\omega|V,\theta)S_e(\omega|H_s,T_z)d\omega \tag{17}$$

Let R denote the local maxima of the Gaussian stress signal X in a sea state. The distribution of R can be described by Rice's distribution function:

$$F_R(r) = \Phi\left(\frac{r}{\varepsilon\sigma_x}\right) - \sqrt{1-\varepsilon^2}\Phi\left(\frac{\sqrt{1-\varepsilon^2}}{\varepsilon}\frac{r}{\sigma_x}\right)e^{-\frac{1}{2}\left(\frac{r}{\sigma_x}\right)^2} \tag{18}$$

where Φ is the standard normal cumulative distribution function, σ_x is the standard deviation of X and $\sigma_x = \sqrt{\lambda_0}$, ε is the spectral width parameter. If $\varepsilon = 0$, Eq. (18) becomes Rayleigh distribution:

$$F_R(r) = 1 - e^{-\frac{r^2}{2\sigma_x^2}}, \quad \text{where } r \geq 0 \tag{19}$$

For the narrow-band Gaussian process, the number of local maxima can be computed through the zero-up crossing frequency of the signal $X(t)$ as $f_z = \frac{1}{2\pi}\sqrt{\frac{\lambda_2}{\lambda_0}}$.

Since the waves in a stationary sea state are actually random processes, the stress cycle range S is also a random variable with the probability density function (pdf) denoted by $f_S(s)$. Then, the

expected value of S^k is computed by $E[S^k] = \int_0^\infty s^k f_s(s)ds$. For a zero mean narrow band Gaussian stress $X(t)$, the stress cycle range S is approximated by two times the stress amplitude R, i.e. $S \approx 2R$. Subsequently, by means of Eq. (19), $E[S^k]$ can be computed by:

$$E[S^k] \approx \int_0^\infty (2r)^k f_R(r)dr = \left(2\sqrt{2}\sigma_x\right)^k \Gamma(\frac{k}{2}+1) \tag{20}$$

where $\Gamma(x)$ is the gamma function. The expected fatigue damage computed by Eq. (15) becomes:

$$E[D] = \frac{N_0}{\alpha} E[S^k] \approx \frac{N_0}{\alpha}\left(2\sqrt{2}\sigma_x\right)^k \Gamma(\frac{k}{2}+1) \tag{21}$$

where N_0 is the expected number of stress cycles and computed by $N_0 = T \cdot f_z$ for $X(t)$, $t \in [0, T]$. Finally, the expected fatigue damage caused by the narrow band stress $X(t)$ denoted by D_T, is:

$$D_T = E[D] \approx \frac{T}{2\pi\alpha}\sqrt{\frac{\lambda_2}{\lambda_0}}\left(2\sqrt{2\lambda_0}\right)^k \Gamma(\frac{k}{2}+1) \tag{22}$$

Equation (22) is also known as the narrow-band approximation and works quite well even for stress signal with spectral width parameter ε up to 0.5. In this thesis, the parameters of the one-slope *S-N* curve are chosen as $\alpha = 10^{12.76}$ and $k = 3$ according to DNV GL (2014).

3.3 Fatigue crack propagation model

For practical engineering application, the fatigue crack propagation estimation is mainly based on the Linear Elastic Fracture Mechanics (LEFM), e.g., Anderson (2017), Sumi (1998), etc. In this thesis, the LEFM is implemented with a ship's spectral response analysis. It yields a simple but reliable fracture model for crack growth analysis in ship structures. The detailed derivation of the model can be founded in Mao (2014). In the following, some basic equations used in this thesis are briefly described.

The crack propagation analysis is based on the linear elastic fracture mechanics (LEFM) using the stress intensity factor (SIF) K. For most ship steel materials, the crack growth rate da/dN against the SIF range ΔK on log-log scales looks like a sigmoidal curve as in Fig. 14. The fatigue crack propagation predicted by the Paris law can be written as:

$$\frac{da}{dN} = C \cdot \Delta K^m \tag{23}$$

where a is the crack length, C and m are material parameters that can be got from design rules, e.g., BS7910 (2005), ΔK is the SIF range during a stress cycle, and da/dN is the corresponding crack growth rate. For ship structures composed of shell and beam elements, the mode I crack is the most common case. This thesis is limited to this mode using LEFM principles. Thus, the SIF can be written as:

$$K = S_p \cdot f\left(\frac{a}{w}\right)\sqrt{\pi a} \tag{24}$$

where S_p is the stress perpendicular to the crack plane, w is the width of the crack plane and $f\left(\frac{a}{w}\right)$ is a dimensionless parameter in terms of the crack geometry and loading type (Mao 2014).

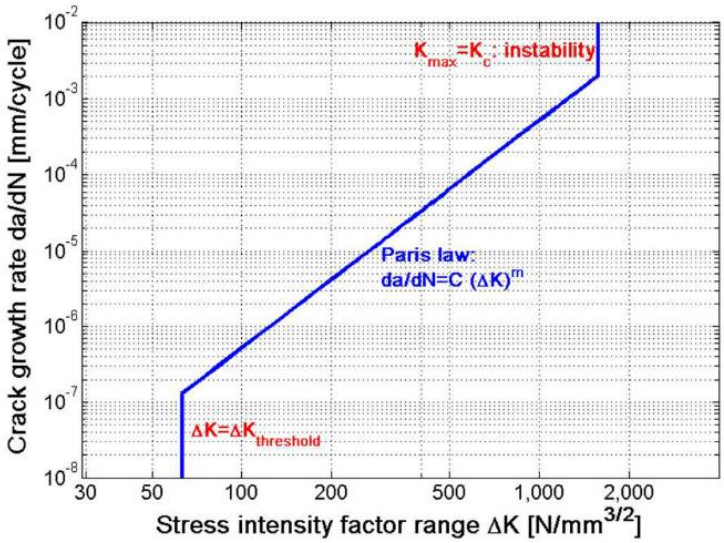

Fig. 14. Simple fatigue crack growth relationship (BS7910 2005).

To predict the fatigue crack propagation due to variable amplitude stresses, a fast and reliable spectral method proposed by Mao (2014) is used for the crack analysis. It is assuming that the crack increment per cycle is small, as the parameter C is very small, while the number of stress cycles in a sea state here is less than a few hundred. The stress response in a stationary sea state is often assumed to be narrow-band Gaussian processes. Then, the expected crack increment under the ith sea state $t \in [T_i, T_{i+1}]$ is computed by:

$$E[\Delta a_i] = C \cdot g^m(a_i) \cdot \frac{\Delta T}{2\pi} \sqrt{\frac{\lambda_2}{\lambda_0}} \Gamma\left(\frac{m}{2} + 1\right) \cdot (2\lambda_0)^{\frac{m}{2}} \tag{25}$$

where $g(a)$ can be computed by a fracture mechanics code, e.g. FRANC2D by Wawrzynek and Ingraffea (1991), ΔT is the time interval for a stationary sea state of $\Delta T = T_{i+1} - T_i$, $\Gamma()$ is the gamma function, λ_0 and λ_2 are the zero- and second-order of the spectral moments of the stress $S_p(t)$ for $t \in [T_i, T_{i+1}]$. The values of λ_0 and λ_2 can be computed by Eq. (17) for ship fatigue assessment.

4 Summary of papers

This chapter summarizes research activities and important results described in the appended papers. All the papers have been categorized into three sections/groups based on their research topics. The first section, **Development of voyage optimization algorithms** starts with a benchmark study in **Paper A** that provides the essence of the voyage optimization algorithms commonly used in the shipping market. The results of **Paper A** indicate the limitations and drawbacks of commonly used voyage optimization algorithms. **Paper B** proposed a newly developed algorithm that overcomes these limitations, and contains other new features, such as course regeneration. Since most trans-ocean vessels are controlled by engine power or RPM rather than speed, **Paper C** adopts an optimization algorithm including both engine power optimization and course optimization for practical sailing operations. The **Uncertainty study** in **Paper D** is also based on the findings of **Paper A**. Uncertainties in the voyage optimization input parameters, such as the metocean forecast and the ship performance model, were not considered in **Paper A**. Thus, **Paper D** conducted several studies to investigate the influence of those uncertainties on the optimization result.

The second section, **Impact of voyage optimization on ship fatigue accumulation**, includes the implementation of voyage optimizations in a ship's operations to mitigate structural fatigue failure and its impact on fatigue assessment during a ship's fatigue design stage. For ship operation, **Paper E** presents the potential benefits of voyage optimization to reduce the risk of ship structural failure due to crack propagation. In **Paper F**, two statistical wave models are compared, and their capability to predict the statistics of waves encountered by ships is validated, proving that actual encountered sea conditions can differ significantly from those provided by design guidelines. In **Paper G**, the impact of ship operations aided by various voyage optimization methods on the wave environments encountered by ships and their consequences on ship fatigue design is presented.

4.1 Development of voyage optimization algorithms

4.1.1 Summary of Paper A

Title: "Benchmark study of five optimization algorithms for weather routing"

Paper A benchmarks five commonly used algorithms to investigate their capabilities for optimum voyage planning with respect to accurate expected time of arrival (ETA), minimum fuel cost and storm avoidance. The advantages and disadvantages of these algorithms, i.e., isochrone, isopone, Dynamic programming, 3D Dynamic programming, and Dijkstra's algorithm, are investigated by implementing and applying these algorithms for the voyage optimization of a 2800TEU containership sailing in the North Atlantic.

In this paper, a modified isochrone algorithm is implemented by dividing a ship's voyage into several sailing stages. At each stage, a ship is assumed to sail at an equivalent time period. Each individual stage begins by varying the ship's heading at each interim waypoint around the reference route, which is the great circle path between the departure and the destination. The isopone algorithm optimizes a ship's route by discretizing a voyage into several stages of equal fuel consumption. This method determines the waypoint of the next stage with minimum fuel by tracing back the headings and speeds.

The dynamic programming method is implemented to search for a local optimum ship sub-route with minimum fuel cost in a pre-defined waypoint/grid system based on the great circle reference path. The ship is assumed to sail at a fixed speed for the entire voyage. The Dijkstra algorithm using the same grid system as in Dynamic programming is applied to find the

optimum ship route. To allow for speed variations along a ship's voyage, a 3D Dynamic programming method is implemented by adding a time dimension in each waypoint in the same pre-defined grid system of dynamic programming method. The method uses the voyage progress as a stage variable through voluntary or involuntary speed/power reduction.

A container ship sailing in the North Atlantic is selected as the case study ship to benchmark these optimization algorithms. Two planning strategies were used for the optimization process, i.e., input parameters, as either fixed power or fixed speed along the ship's voyage. In the fixed-speed-based study, the ship keeps a constant speed during the voyage. In the constant-power-based study, the ship keeps constant power during the voyage and its speed changes due to different weather and sea conditions.

The sailing time and fuel consumption estimated by different optimization algorithms are presented in Table 4. In fixed speed-based voyage optimization, the sailing time and fuel consumption estimated by the isopone method, dynamic programming method, and Dijkstra's algorithm were close to each other. The result given by the isochrone method has a longer sailing time because the node selection criterion was set to the lowest cost.

Table 4. Sailing time estimated by different optimization algorithms.

Optimization methods	**Isochrone**		**Isopone**		**2DDP**		**3DDP**		**Dijkstra**	
	ETA [h]	Fuel [ton]	ETA [h]	Fuel [ton]	ETA [h]	Fuel [ton]	ETA [h]	Fuel [ton]	ETA [h]	Fuel [ton]
Fixed speed	171.8	732.4	166.4	695.6	166.2	695.6	173.4	638.0	166.4	692.7
Fixed power	165.6	702.1	166.0	702.7	165.7	700.3	173.4	638.0	165.6	700.1

In the fixed-power voyage optimizations, the results of sailing time and fuel consumption estimated by all methods except the 3D dynamic programming are quite similar to each other. The 3D dynamic programming yields a longer sailing time and lower fuel consumption because of the speed variations and the voluntary speed reductions during the voyage. The results given by the fixed-power based study gives a smaller estimated sailing time but higher fuel consumption than those given by the fixed-speed based study. This is because the speed in the fixed-power based study is generally higher than the speed in the fixed-speed based study.

The results show that the 3D dynamic programming method has more capabilities (voluntary speed reduction during harsh weather conditions) and better results (saving approximately 8% of fuel) for voyage planning. The 3D dynamic programming method was able to reduce speed when encountering a storm.

4.1.2 Summary of Paper B

Title: "A three-dimensional Dijkstra's algorithm for multi-objective ship voyage optimization"

The study of **Paper A** lists the limitations and drawbacks of those conventional voyage optimization algorithms, i.e., unable to provide globally optimal ship routes if one allows for speed/power variations along the voyage, unable to conduct multi-objective optimization, etc. Therefore, in **Paper B,** a new method is developed to allow for both global optimization capability and multi-objective optimization.

In this method, a 3D graph/grid system is firstly generated whose nodes/waypoints are created with the information of geometric points in the voyage and the time set. The edges/sub-paths are then generated by the adjacent nodes/waypoints, considering the constraints during the voyage. The edges/sub-paths are assigned with weights based on weather information and cost function (the ship performance model). Finally, Dijkstra's algorithm is implemented in the 3D graph/grid system to search candidate optimum routes with a series of ETAs.

The full-scale measurements of a 2800TEU container ship sailing in the North Atlantic are used as a comparative reference in the case study to demonstrate the capability of the proposed 3D Dijkstra's algorithm (3DDA). The optimization results of the 3DDA are also compared with the results from other sailing approaches, i.e., the 2D Dijkstra's algorithm (2DDA) and the great circle sailing. The case study voyages are divided into eastbound voyages and westbound voyages and the results are shown in the following Table 5 and 6.

For eastbound voyages, shipping operators may not seriously consider voyage optimization, since storms in the North Atlantic always move from the west to the east. However, the results show that the 3DDA method has also a great potential of saving fuel up to about 12% in comparison with the ship's actual eastbound sailing routes. For westbound voyages, the 3DDA method can always provide a route with averagely 12% of the fuel-saving in comparison with the actual sailing for a given ETA.

Table 5. Results of various voyage optimizations for the eastbound voyages.

Voyage name	Optimization methods	ETA [h]	Fuel consumption [ton]	Distance [km]
20080117	Actual route	90.8	249.8	3193.6
	Great circle	90.6	235.8	3130.4
	2DDA	90.5	239.7	3186.8
	3DDA	91.0	230.6	3136.9
20080523	Actual route	88.7	229.0	3176.2
	Great circle	88.6	220.5	3127.2
	2DDA	88.8	221.7	3164.8
	3DDA	89.0	220.4	3135.3
20081224	Actual route	94.7	246.4	3238.8
	Great circle	94.6	218.6	3132.1
	2DDA	94.5	222.9	3196.9
	3DDA	94.5	216.7	3132.1

Table 6. Results of various voyage optimizations for the westbound voyages.

Voyage name	Optimization methods	ETA [h]	Fuel consumption [ton]	Distance [km]
20080129	Actual route	105.8	309.8	3354.2
	Great circle	105.6	304.5	3168.1
	2DDA	106.2	301.2	3429.2
	3DDA	106.0	286.2	3270.9
20080218	Actual route	94.5	280.7	3191
	Great circle	94.5	272.0	3121.3
	2DDA	94.4	275.1	3196.5
	3DDA	94.5	269.0	3142.0
20080424	Actual route	92.5	314.3	3244.0
	Great circle	92.5	246.1	3129.9
	2DDA	93.2	245.7	3241.8
	3DDA	92.5	243.8	3136.4
20081214	Actual route	104.8	301.7	3186.7
	Great circle	105.3	272.5	3114.5
	2DDA	104.5	278.2	3329.1
	3DDA	105.0	262.2	3193.4

Through the comparison with other voyage optimization methods, it shows that the 3DDA method can provide better voluntary speed reduction or speed increase. This method has a big potential to lower the ship's fuel consumption and plan the sailing schedule with a more accurate expected time of arrival. It is shown that the 3DDA method can help to reduce on average about 10% fuel consumption for all the investigated voyages involved in the case study, while still keep the same ETAs as the measured voyages. Meanwhile, other capabilities of the proposed method, i.e., multi-objective optimization and fast course regeneration & weather updating are also discussed in the paper.

4.1.3 Summary of Paper C

Title: "A ship engine power-based voyage optimization method by combing genetic algorithm and dynamic programming concepts"

Course optimization is widely adopted by conventional voyage optimization algorithms. More complex voyage optimization algorithms, such as 3D Dynamic programming in **Paper A** and 3D Dijkstra's algorithm proposed in **Paper B**, concern speed optimization for further improvement of the optimization results. However, under the rapid-change environmental conditions in open sea areas, a ship's speed is difficult to be accurately controlled. Moreover, ships such as tanker ships, bulk carriers who don't have strict required time of arrivals are often controlled by shaft power or RPM. Researches related to engine power optimization are very seldom because of the complex iteration to solve the relationship between settled engine power and ship speeds under changing sea environments during the optimization process. In **Paper C**, a voyage optimization method under the scheme of genetic algorithm is proposed by taking discrete engine powers as inputs. It should be noted that the method proposed in **Paper C** is not an improved version of the one in **Paper B**. It introduces an approach for solving shaft power optimization problem.

The scheme of the proposed method is divided into two parts, i.e., the *decision vector generator* part and the *implementation of the genetic algorithm* part. The decision vector generator is used to generate decision vectors. A decision vector represents both the trajectory of a ship route and its corresponding shaft power configuration. The decision vector is used as an individual sample in the genetic algorithm. To increase the efficiency of the convergence and prevent early local convergence, three types of decision vector generators are used:

1) Heuristic decision vector generator (HDVG).
2) Deterministic decision vector generator (DDVG).
3) Stochastic decision vector generator (SDVG).

The HDVG uses Dijkstra's algorithm to generate optimal trajectories with constant shaft power settings. It is used to confine the search space for the genetic algorithm to improve the efficiency of the convergence. DDVG is used to generate shaft power configurations for certain routes by using a dynamic programming approach. In SDVG, a stochastic approach is used to generate random decision vectors including both the routes and their corresponding shaft power configurations.

Several case study voyages with full-scale measurements when a chemical tanker ship was sailing in the North Atlantic during the year 2015 and 2016 are used to demonstrate the capacities of the method. Three different route planning methods are taken for the comparison:

1) The actual sailing routes from the full-scale measurements.
2) The results from the heuristic method.
3) The results from the proposed method.

The case study voyages are divided into eastbound voyages and westbound voyages. Through the comparison, the proposed method shows the capability of fuel-saving with averagely 5.2%

and 3.4% compared with the actual sailings and the heuristic routes respectively. In particular, the proposed method is outperforming other route planning methods under extreme environmental conditions. In the eastbound voyage 20160317 shown in Fig. 15, the ship sailing along the actual route encountered two storms and the optimal route helps avoid the storms. In the middle of the voyage, the actual route encountered harsh weather conditions with significant wave height up to 10 meters. In this extreme case, the proposed method saves fuel up to approximately 14.5% compared to the actual sailing route while keeping the accurate ETA.

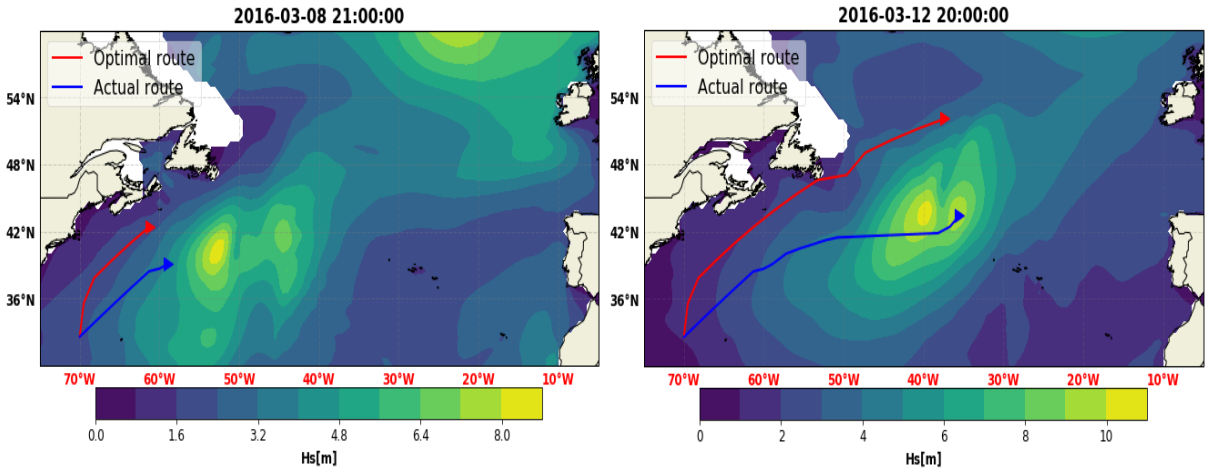

Fig. 15. Contour plot of significant wave height H_s for the voyage 20160307.

4.1.4 Summary of Paper D

Title: "Effectiveness of 2D optimization algorithms considering voluntary speed reduction under uncertain metocean conditions"

Algorithms presented in **Paper B** and **Paper C** are developed under the assumption that the input parameters such as weather data and ship models are accurate. However, large uncertainties existed in these input parameters of voyage optimization algorithms. Meanwhile, due to the limited accepted waiting time from ship operators to perform a voyage optimization, the weather routing market is more willing to adopt two-dimensional voyage optimization algorithms for voyage planning.

In **Paper D**, an uncertainty study for minimum fuel is conducted for two-dimensional voyage optimization algorithms including a course optimization algorithm and a new-proposed speed optimization algorithm, which consider the voluntary speed reduction along a fixed sailing route. The uncertainty study includes the influence of the uncertainties from the weather forecast, ship performance models and operational strategies. Due to the complexity and imperfection of the physical description in today's weather forecast models, the weather forecast data is inevitably including large uncertainties. Consequently, the accuracy of the objective function in the voyage optimization algorithm determined by the weather forecast data is uncanny. In the study of the uncertainties in weather forecast, weather hindcast data is used to investigate the impact of the uncertainties from the weather forecast data on the optimization results. Meanwhile, the objective function in the voyage optimization is defined by the ship performance models. Two ship fuel consumption models, the Kwon's model, and a semi-empirical model are used to study the uncertainties from the ship model. In addition, slow steaming is a common operation strategy today to minimize a ship's fuel consumption when sailing at sea. Longer sailing time brings more uncertainties for voyage optimization in terms of slow steaming. The operational strategy, slow steaming is also concerned in the uncertainty

study. The full-scale measurement of the ship's operation at sailing in the North Atlantic during the year 2009 is used as a reference in this study. To analyse sensitivities and robustness of two-dimensional voyage optimization algorithms due to inputs uncertainties, three different voyage planning approaches are compared with the actual sailing routes in the case study:

1) The great circle routes with fixed speed (Great Circle sailing).
2) The routes from constant speed course optimization (CS course optimization).
3) The routes from great circle speed optimization (GC speed optimization).

This study mainly investigates the impact of uncertain weather forecast inputs on a ship's voyage optimization solutions. The voyages are divided into westbound voyages and eastbound voyages. The sailing distance, sailing time (ETA), forecast fuel consumption and actual fuel consumption for all these investigated voyages are listed in Table 7 and Table 8 for all the westbound voyages and eastbound voyages respectively. For the westbound voyages, the three investigated voyage optimization/planning methods behave generally better than the ship's actual sailing in terms of fuel consumption. In particular, the GC speed optimization method generates better results for most of the voyages based on weather forecast information. For the eastbound voyages, the GC speed optimization method can produce the best results of voyage planning in terms of minimum fuel consumption in the three out of four chosen eastbound voyages. In comparison with actual sailing, it can save about 7.5% of fuel. In comparison with the CS course optimization methods, it can save about 2.5%-3% of fuel-dependent on if the weather forecast or hindcast data is used for the analysis.

Table 7. Results of optimized routes by various optimization methods for 5 westbound voyages.

Voyage name	Voyage strategy	Distance (km)	ETA (hours)	Forecast fuel (ton)	Hindcast fuel (ton)
20090105	Actual sailing	3000	93.0	187.6	188.7
	Great Circle sailing	2920	92.7	146.8	150.4
	GC speed optimization	2920	93.0	146.5	150.0
	CS course optimization	3004	92.7	154.3	155.4
20090202	Actual sailing	4223	138.5	454.8	477.5
	Great Circle sailing	3546	138.3	431.0	470.9
	GC speed optimization	3546	138.6	410.4	432.4
	CS course optimization	3924	137.9	372.5	445.4
20090604	Actual sailing	3233	93.0	229.0	232.5
	Great Circle sailing	3135	92.7	213.2	214.0
	GC speed optimization	3135	93.0	211.2	212.3
	CS course optimization	3265	92.5	222.0	223.6
20091119	Actual sailing	2722	89.0	175.2	176.2
	Great Circle sailing	2710	88.2	180.7	181.6
	GC speed optimization	2710	89.1	171.7	176.2
	CS course optimization	2867	87.8	182.8	184.9
20091218	Actual sailing	2922	98.0	206.5	222.4
	Great Circle sailing	2877	97.9	193.8	205.7
	GC speed optimization	2877	98.1	191.5	204.5
	CS course optimization	3003	97.9	206.0	220.1

Table 8. Results of optimized routes by various optimization methods for 4 eastbound voyages.

Voyage name	Voyage strategy	Distance (km)	ETA (hours)	Forecast fuel (ton)	Hindcast fuel (ton)
20090121	Actual sailing	3537	100.5	299.4	338.9
	Great Circle sailing	3150	100.1	298.5	354.9
	GC speed optimization	3150	100.5	273.7	329.1
	CS course optimization	3353	99.7	263.9	311.9
20090618	Actual sailing	3172	92.0	196.9	199.2
	Great Circle sailing	3091	92.0	184.5	188.5
	GC speed optimization	3091	92.1	183.9	187.6
	CS course optimization	3184	92.1	188.8	190.9
20091129	Actual sailing	2781	88.0	159.3	159.3
	Great Circle sailing	2741	87.9	145.7	148.6
	GC speed optimization	2741	87.9	145.3	144.3
	CS course optimization	2796	88.3	148.5	152.4
20091228	Actual sailing	2903	87.0	212.8	234.7
	Great Circle sailing	2859	86.6	202.6	221.0
	GC speed optimization	2859	87.0	200.0	217.2
	CS course optimization	2908	86.1	205.3	223.4

In this paper, weather uncertainty on voyage optimization for slow steaming operations is also discussed. For most of the voyage, the great circle speed optimization method can generate better routes in terms of fuel-saving for the slow steaming operations.

4.2 Impact of voyage optimizations on ship fatigue accumulation

4.2.1 Summary of Paper E

Title: "Voyage optimization for mitigating ship structural failure due to crack propagation"

In **Paper E**, the impact of different ship voyage planning methods on ship fatigue crack propagation is investigated. It presents the potential application of voyage optimization to reduce the fatigue crack propagation rate. In this paper, the voyage optimization algorithms introduced in **Paper A** are further categorized into two groups, dynamic-grid-based methods, and static-grid-based methods. To study the benefits of voyage optimization systems on the reduction of fatigue crack propagation in ship structures, i.e., a potential extension of sailing life before crack repairs are required, voyage optimization methods are combined with a linear elastic fracture mechanics model which could predict the crack propagation speed in ships. In this paper, a 2800TEU container ship sailing in the North Atlantic with an initial crack length assumed to be 100 mm is assumed for the demonstration analysis.

This study compares the crack propagations if the vessel were sailing along four planned ship routes, i.e., the great circle, routes optimized by the Isochrone and dynamic programming methods, and the measured original sailing routes. All ship routes were expected to reach the destination at approximately the same time (ETA as measured). The crack propagation results plotted in Fig. 16 shows a great reduction of crack propagation when using optimization algorithms in comparison with the conventional great circle sailing routes. The great circle routes are the shortest paths for these voyages, but the rate of fatigue crack propagation along these routes is much faster than those for other route planning methods. The benefit of the reduction of fatigue crack propagation in ship structures or sailing life extension is quite significant, i.e., with a maximum life extension of 100% in this case study.

In addition, this paper compares the benefits of using voyage optimizations when sailing in different directions, i.e., between eastbound and westbound voyages. The benefits of implementing a voyage optimization to aid a ship's operation are not obvious for eastbound voyages in the North Atlantic, especially during summer seasons. In some winter voyages, crack propagation can be reduced by more than 50% if sailing along routes recommended by these optimization algorithms. This is because, in the North Atlantic, storms with severe metocean conditions always move from west to east and provide much potential for route planning to avoid these storms. The following sea operations do not cause as serious fatigue problems as the head sea operations.

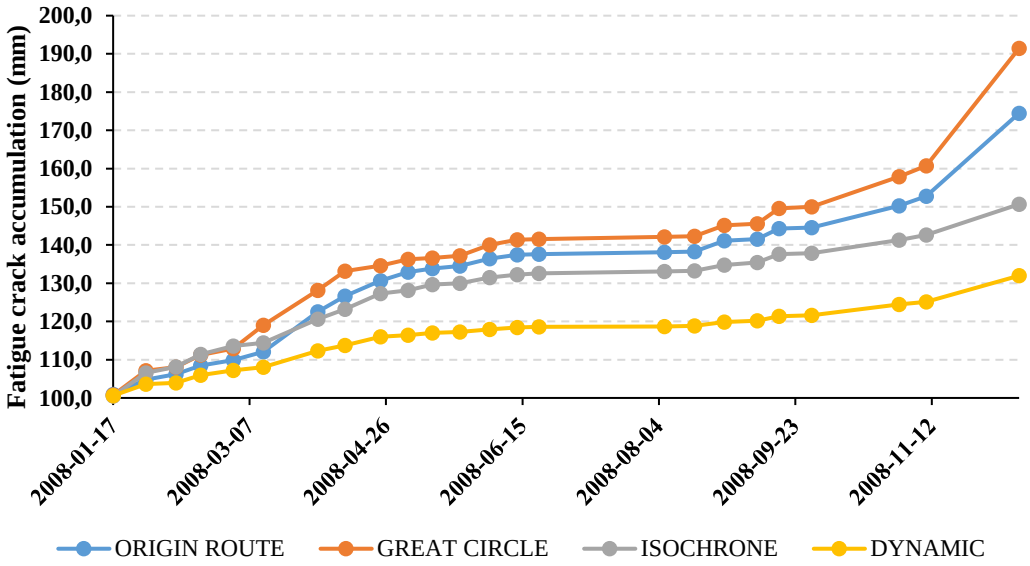

Fig. 16. Accumulated fatigue crack length with different route planning methods.

4.2.2 Summary of Paper F

Title: "Comparison of two statistical wave models for fatigue and fracture analysis of ship structures"

In a ship's design process, the wave-induced loads on the vessel are needed to be estimated by the wave scatter diagram issued by the classification societies. However, the actual wave environment encountered by individual ships may be not consistent with that provided by the classification societies that are unlikely to consider operational conditions for individual ships. In **Paper F**, two statistical wave models based on hindcast data and satellite wave measurements are introduced and compared with the wave statistics from classification guidelines and the wave measurements carried out by onboard radar. The two statistical wave models include a wave storm model which is based on wave scatter data extracted from the reanalysis dataset along ship routes and a statistical spatio-temporal wave model. The wave storm model is established through several steps of fitting to Weibull distributions, while the spatio-temporal model is based on the spatio-temporal correlation of wave from reanalysis and satellite measurements.

A 2800TEU containership equipped with a hull-monitoring system is used to check the reliability of the two wave models. First, the wave statistics from the two statistical models are compared with reanalysis data and classification guidelines. It shows that the variation of onboard measured H_s can be well reflected by the reanalysis data, while using wave statistics from class guidelines may overestimate 100% of the ship's fatigue damage. Second, the procedure of simulating the wave-induced structural stresses is calibrated and validated. It

shows that the characteristic of stress variations in the two generated stress signals agrees well with that of the measured stresses.

In this paper, the capability of two statistical wave models to emulate the random nature of the waves is validated. First, the natural variability of the wave environment is simulated by the spatio-temporal and the storm wave model. It shows that the statistical variability can be well captured by the two models. Second, the statistical quantities of H_s simulated from the two wave models are further examined by the estimation of the first three moments of H_s. The first three moments of H_s are estimated and listed in Table 9. In Table 9, the significant wave height signals are coming from three different sources, i.e., extracted from ECMWF ERA5 hindcast dataset for the same location as the measured routes but with a varying year from 2000 to 2015, simulated 100 times of H_s along the measured ship routes from the storm model and the spatio-temporal model. Table 9 shows that the wave statistics estimated from both the spatio-temporal model and the storm model agree perfectly well with the ERA5 extracted H_s. In addition, the wave models are proved to have the capability of predicting H_s of several waypoints conditionally on the given wave information surrounding the waypoints along the same ship routes.

Table 9. Various moments of H_s as a random variable simulated by statistical wave load models.

Yearly statistics of H_s	**ERA5 15-year data**		**Storm model**		**Spatio-temporal model**	
	Mean	std	Mean	std	Mean	std
First moment E[H_s]	3.00	0.15	2.91	0.09	3.03	0.10
Second moment E[H_s^2]	11.52	1.41	10.78	0.90	11.58	0.92
Third moment E[H_s^3]	55.25	12.03	49.38	8.43	55.06	8.33

After proving the capabilities of two statistical wave load models to emulate the random nature of the waves, the application of the two wave models for ship fatigue assessment is demonstrated. First, the ship's operational wave environments and corresponding stress signals are generated. Then, the high cycle fatigue damage is estimated for those generated stresses. Finally, the structural detail is simplified and an initial crack length is assumed to be 22mm. The crack propagations under these generated stress signals are estimated by the FASTRAN code. The damages and crack propagations are compared with those estimated from the measured stress signals. The mean and standard deviation of accumulated fatigue damages and the total crack growth for 1 year that are estimated from different generated stress signals are presented in Table 10. Table 10 indicates both the spatio-temporal wave model and the storm model can describe well the wave variation encountered by ships and confirms the benefits of using a weather routing service to avoid encountering harsh sea environment.

Table 10. Fatigue damage estimated by *S-N* method and crack propagation estimated by FASTRAN code under different stresses during one-year ship sailing routes.

The way to get the stress signals	***S-N* fatigue damage**		**Crack propagation [mm]**	
	Mean	STD	Mean	STD
Measured stresses	0.0133		23.65	
Simulated using ERA5 H_s of same year	0.0146		24.05	
Simulated using ERA5 H_s of 15 years	0.0132	0.0025	24.17	0.42
Simulated using Spatio-Temporal Model H_s	0.0138	0.0014	24.59	0.53
Simulated using the Storm Model H_s	0.0234	0.0040	26.73	0.79

4.2.3 Summary of Paper G

Title: "Impact of voyage optimizations aided operation on a ship's fatigue design"

Paper G investigates the impact of various voyage optimizations used in assist a ship's operations on the long-term wave statistics and corresponding fatigue life between design and operational conditions. It lists the factors that can affect the fatigue design based on stress-based approaches. Fatigue estimation relies on long-term wave statistics, which are normally provided by classification guidelines. However, different ship operations such as slow steaming and voyage-optimization-aided operations could greatly affect the encountered wave statistics and thus affect the ship's fatigue life.

In this paper, the wave scatter diagram from classification society guidelines (IACS 2010) used for ship fatigue design is used as a reference for comparison with the wave statistics during a ship's operations assisted by different voyage optimization methods, which can lead to optimized routes with "better" planned calm sea environments.

To study the impact of voyage-optimization-aided ship operation on the long-term statistics of waves encountered by ship, three years of full-scale measurements from a 2800TEU container ship equipped with a hull-monitoring system are used. The hull monitoring system installed on the studied ship has an old conventional weather routing system using the so-called Isochrone method for voyage optimization, in order to guide the ship's navigation to avoid severe wave environment conditions. The ship was operated in the North Atlantic for transportation between Europe and North America.

All the encountered wave conditions during the three-year-measurement campaign are extracted and statistically processed. The IACS-suggested wave scatter diagram for North Atlantic operation is presented as well for the comparison, shown in Fig. 17, which shows that the studied ship has planned safer routes and avoided extremely harsh sea areas, compared to the IACS guidelines.

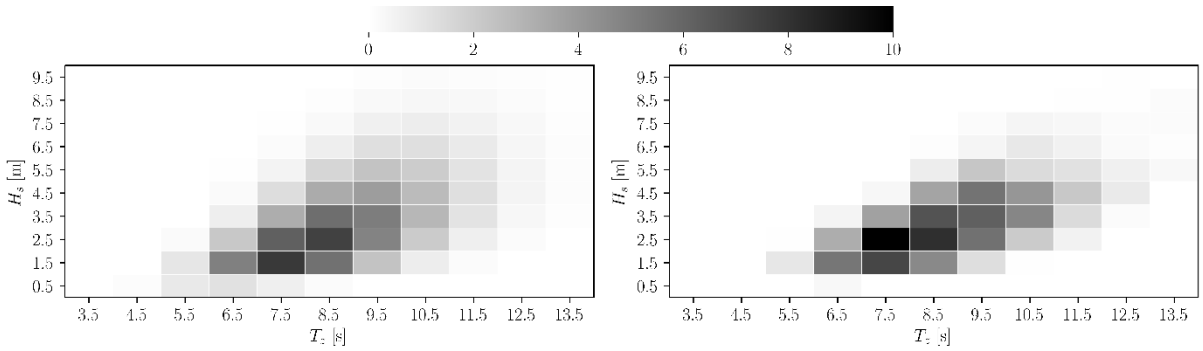

Fig. 17. Wave scatter diagram comparison for (a) IACS North Atlantic operation guideline, (b) actual measurements from the studied container ship; the color bar presents the probability of occurrence.

To demonstrate the voyage optimization influence on wave statistics, the short-term encountered wave environments from four planned sailing routes of the case study ship are compared: 1) the actual routes; 2) the routes with minimum damage; 3) the routes with minimum fuel consumption; 4) the Great Circle routes. Routes 2 and 3 are optimized by the voyage optimization algorithm proposed in **Paper B**. Fig. 18 shows the fatigue damage accumulations over three-year sailing in North Atlantic by different ship operations. It shows that the fatigue life can be effectively extended by at least 50% by voyage optimizations.

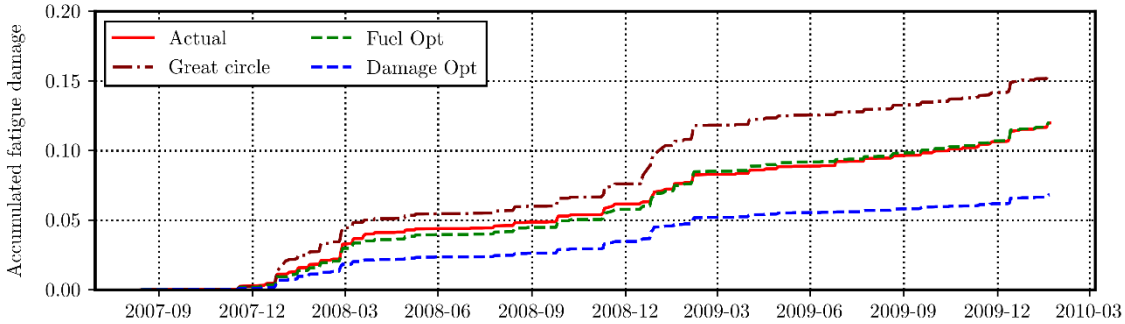

Fig. 18. Fatigue damage accumulations for different ship operations over three years.

5 Conclusions

Voyage optimization recognized as one of the most effective ways to improve ships energy efficiency and safety has been widely implemented in the current shipping industry (DNV GL 2015). The main objective of this thesis is to develop new voyage optimization algorithms to reduce a ship's fuel consumption and air emission, as well as ensure reliable expected time of arrival (ETA) during a ship's operations. In addition, this thesis also aims at studying the impact of voyage optimization aided ship operations on the wave environments encountered by ships and corresponding ship fatigue design. The innovative voyage optimization algorithms developed in this thesis have addressed the improvement of the state-of-art voyage optimization algorithm, and providing additional capabilities and features such as globally optimal solutions and multi-objective optimization capability. The application of voyage optimization to aid a ship's operations for mitigating the risk of structural failure mainly focuses on reducing the crack propagation and fatigue damage accumulation in ship structures, leading to the extension of a ship's service life with respect to fatigue safety.

The results presented in the appended papers showed scientific developments in the areas of voyage optimization algorithms with respect to increased ship energy efficiency and enhanced safety during ship operations, as well as the impact of their application to a ship's fatigue design. The thesis: 1) illustrates the essence of commonly used voyage optimization algorithms (strengths and weaknesses), 2) develops two advanced voyage optimization algorithms for fuel-saving, which cover most ship control operations (speed operation and engine power operation), 3) demonstrates the impact of uncertain input parameters on two-dimensional voyage optimization algorithms, and 4) investigates the impact of voyage optimization aided operations on a ship's fatigue design.

The main findings and conclusions are presented below, as part of the sub-goals presented in Section 1.5.

The essence of the commonly used voyage optimization algorithms

Paper A drew the conclusion that Dijkstra's algorithm and the dynamic programming method are used in a predefined waypoint/grid system, and both can find the best route from a predefined waypoint/grid system. The solution accuracy is highly dependent on the grid resolution. The advantage of using a predefined grid system is that it can easily handle impassable areas.

Another finding in **Paper A** is that the isochrone and isopone methods are more suitable for single-objective optimization. The 3D dynamic programming method is more capable of analyzing dynamic weather, essential for both voluntary and involuntary speed reduction.

The development of new voyage optimization algorithms

Papers B and **C** proposed two innovative voyage optimization algorithms, i.e., a 3D Dijkstra's algorithm and a ship engine power-based voyage optimization method combining various optimization algorithms. The 3D Dijkstra's algorithm proposed in **Papers B** is applied for ship operations through a series of optimum sailing speeds as navigation control inputs. It was found that the 3D Dijkstra's algorithm can help reduce fuel consumption by an average of approximately 10% compared with actual sailing routes while maintaining the planned ETAs. It was concluded that the 3D Dijkstra's algorithm is also capable of multi-objective optimization (minimum fuel consumption, ETA and lowest fatigue damage) with Pareto front analysis. Additionally, it can regenerate routes with little effort. This method can provide better voluntary speed reduction or speed increases for energy-efficient shipping route planning.

The optimization method proposed in **Paper C** is applied to ship operations through a series of optimum engine powers as navigation control inputs. It introduced a scheme for solving this problem by combining genetic algorithm and dynamic programming concepts. It was shown that the method can provide an average of 5.2% fuel savings compared with actual sailing routes and 3.4% over routes optimized with fixed shaft power settings.

Impact of the input parameter uncertainties

Paper D studied the uncertainties in voyage optimization results originated from the voyage optimization input parameters, i.e., the ship performance models, the metocean forecast, the voyage optimization algorithms and operational strategies. The results showed that using different ship energy performance models for two-dimensional voyage optimization algorithms can produce 4-10% deviations in fuel consumption estimates. A 3-10% fuel consumption difference is expected from the metocean forecast uncertainties for the same voyage optimization method. It was also concluded that sailing through the Great Circle routes with the proposed speed optimization algorithm is a better option, especially for slow steaming operations, compared with course optimization at a fixed speed.

Reduction in fatigue crack growth rate in the ship structure

In **Paper E**, the impact of using voyage optimization during the ship's operational period on crack propagation is investigated. It was found that commonly used voyage optimization algorithms can help the ship avoid severe storm conditions, leading to diminished fatigue crack propagation with enhanced ship structural integrity. The dynamic programming method can help increase vessel fatigue service time by at least 50%.

Impact of different ship voyage optimizations on encountered wave environments and ship fatigue design

In **Paper F**, two statistical wave models, i.e., the wave storm model and the spatio-temporal wave model, were compared. It was validated that both wave models can well describe the wave statistics of the ship's encountered sea environments. Additionally, it was concluded that the two wave models can be used to estimate the stress signals for the ship structural details and analyze fatigue damage accumulation and crack propagation for specific ship voyages. It was shown that these models have great potential to provide wave statistics for more realistic ship fatigue design.

In **Paper G**, it was shown that the wave statistics provided by the classification guidelines for ship design purpose gives a harsher prediction of the encountered wave conditions compared with the encountered wave statistics of the actual sailings. Furthermore, the difference in wave statistics from various optimization methods is about 10-30%, while the difference in fatigue damage accumulation is more than 50%. It was concluded that the ship operations aided by the voyage optimization can influence the wave statistics and consequently influence the ship fatigue life which can be extended by at least 50% when using voyage optimization.

6 Future work

Voyage optimization for long voyages

Today's metocean forecast institutes mostly provide 10 day forecast data to the end-users. It is difficult for voyage optimization algorithms to provide realistic solutions for long voyages with total sailing time more than 10 days in the future. Thus, innovative optimization algorithms should be developed to provide optimal route solutions for these long voyages.

Impact of updating metocean forecast data during voyages on voyage optimization results

The voyage optimization process is usually conducted before the departure of a voyage. The metocean forecast data is usually updated every 6 or 12 hours. When a ship has the metocean forecast data updated during the voyage, it can either follow the original route plan or re-optimize the plan. It is essential to investigate the impact of updating the route plan during the voyage compared with the original route plan.

Voyage optimization considering transient ship states

A long-term focus should also address how to consider a ship's transient states in voyage optimization algorithms, such as various ship motions and trim variations. Most voyage optimization problems are solved in discrete forms, and their objective functions normally describe the mean ship state during a period (hours), such as fuel consumption rate and fatigue damage accumulation rate. Thus, the cost of a discrete form along a candidate route can be calculated. It is confusing to consider a ship's transient state as an objective to be estimated in a discrete form voyage optimization problem. However, it is essential to determine a ship's transient state during a voyage. Thus, an appropriate approach is needed for this problem.

Development of the ship performance model

A ship's performance models are key elements affecting the voyage optimization results. In the present study, the ship power/fuel consumption models include semi-empirical models, theoretical models, and basic statistical models to fit the residual between the measured performance and that predicted by theoretical models. These approaches provide a good estimate of power/fuel consumption, but they are not sufficiently accurate. Therefore, another area for future work is to combine theoretical modeling with machine learning algorithms to update a ship's performance models in real-time.

References

Alexandersson, M. (2009). A study of methods to predict added resistance in waves, Master thesis, Report number 2296, Royal Institute of Technology, Stockholm, Sweden.

Anderson, T. L. (2017). Fracture Mechanics: Fundamentals and Applications, Fourth Edition, CRC Press, Taylor and Francis Group, ISBN 9781498728133.

Andersson, A. (2015). Multi-objective optimization of ship routes, Master's thesis, Department of Applied Physics, Chalmers University of Technology, Gothenburg, Sweden.

AGCS. (2019). Safety and shipping review 2019, http://www.agcs.allianz.com/. [Accessed: 2020-03-14.]

Ballou, P., Chen, H. and Horner, J. D. (2008). Advanced methods of optimizing ship operations to reduce emissions detrimental to climate change, OCEANS 2008, Quebec City, QC, 2008, pp. 1-12.

Bellman, R. (1952). On the Theory of Dynamic Programming. Mathematics, Vol. 38, pp. 716-719.

Bowditch, N. (2002). The American Practical Navigator. National Imagery and Mapping Agency. Bethesda, Marland, USA.

BS 7910. (2005). Guide on methods for assessing the acceptability of flaws in metallic structures, British Standards Institution, UK.

Calvert, S. (1990). Optimal weather routeing procedures for vessels on trans-oceanic voyages. PhD thesis, Polytechnic South West, UK.

Chen, H. (1978). A dynamic program for minimum cost ship routing under uncertainty, PhD thesis, Dept. of Ocean Engineering, Massachusetts Institute of Technology, USA.

Chen, H. (2013). Voyage Optimization Supersedes weather routing, Jeppesen Commercial Marine Journal.

De Wit, C. (1990). Proposal for low cost ocean weather routeing, Journal of Navigation, Vol. 43(3), pp. 428-439.

Dijkstra, E.W. (1959). A note on two problems in connexion with graphs, Numerische Mathematik, Vol. 1, pp. 269–271.

DNV GL. (2014). Fatigue Assessment of Ship Structure, Classification Note No.30.7.

DNV GL. (2015). Energy Management Study 2015, www.dnvgl.com, Høvik, Norway. [Accessed: 2020-03-14.]

Dorigo, M., Manizzzo, V., and Colomi, A. (1991). Ant system optimization by a colony of cooperating agents. IEEE Transaction on System, Man and Cybernetics- Part B: Cybernetics, Vol. 26(1), pp. 29-41.

Fricke, W., Cui, W., Kierkegaard, H., et al. (2002). Comparative fatigue strength assessment of a structural detail in a containership using various approaches of classification societies. Marine Structures, Vol.15, pp. 1-13.

GAC-SMHI (2020). https://www.gac.com/services/shipping/weather-routing/. [Accessed: 2020-03-14.]

Hagiwara, H. (1989). Weather routing of (sail-assisted) motor vessels, PhD thesis, Delft University of Technology, Delft, The Netherland.

Hinnenthal, J. (2008). Robust Pareto optimum routing of ships utilizing deterministic and ensemble weather forecasts, PhD thesis, Technischen Universität Berlin, Berlin, Germany.

Holtrop, J. and Mennen, G.G.J. (1984). An approximate power prediction method, International Shipbuilding Progress, Vol. 31, pp. 166-170.

IACS (2010). Unified Requirements concerning Strength of Ships, Rev. 7. International Association of Classification Societies.

IMO (1999). Annex 25 Guidelines for Voyage Planning resolution A.893(21), SOLAS (Chapter 5), Safety of Navigation.

IMO (2016). Study on the optimization of energy consumption as part of implementation of a ship energy efficiency management plan.

ISO (2015). Ships and marine technology – Guidelines for the assessment of speed and power performance by analysis of speed trial data, ISO 15016.

James, R. (1957). Application of wave forecast to marine navigation, US Navy Hydrographic Office, Washington.

Klompstra, M.B., Olsde, G.J. and Van Brunschot, P.K.G.M. (1992). The isopone method in optimal control, Dynamics and Control, Vol. 2(3), pp. 281-301.

Kwon, W., Suh, I.H., Lee, S. and Cho, Y. (2007). Fast reinforcement learning using stochastic shortest paths for a mobile robot, Proceedings of the 2007 IEEE/RSJ International Conference on Intelligent Robots and Systems, Oct. 29-Nov. 2, San Diego CA., pp: 82-87.

Kwon, Y. J. (2008). Speed loss due to added resistance in wind and waves, Naval Architect (2008), pp.14-16.

Larsson, E., Simonsen, M.H. and Mao, W. (2015). DIRECT Optimization algorithm in weather routing of ships, Proceeding of the 25th ISOPE, Hawaii, USA.

Lee, S.M., Roh, M.I., Kim, K.S., Jung, H., Park, J.J. (2018). Method for a simultaneous determination of the path and the speed for ship route planning problems, Ocean Engineering, Vol.175, pp. 301-312.

Lin, Y. H., Fang, M. C., and Yeung, R. (2013). The optimization of ship weather-routing algorithm based on the composite influence of multi-dynamic elements, Applied Ocean Research, Vol. 43, pp. 184-194.

Liu, S., Shang, B., Papanikolaou, A. and Bolbot, V. (2016). Improved formula for estimating added resistance of ships in engineering applications, Journal of Marine Science and Application, Vol.15, pp. 442-451.

Maki, A., Akimoto, Y., et al. (2011). A new weather-routing system that accounts for ship stability based on a real-coded genetic algorithm, Journal of Marine Science and Technology, Vol.16, pp. 311–322.

Mao, W. (2010). Fatigue assessment and extreme response prediction of ship structures, Doctoral thesis, Chalmers University of Technology, Gothenburg, Sweden.

Mao, W, Ringsberg, J.W. and Rychlik, I. (2010). Development of a fatigue model useful in ship routing design, Journal of Ship Research, Vol. 54(4), pp. 281-293

Mao, W., Li, Z., Ringsberg, J.W. and Rychlik, I. (2012). Application of a ship routing fatigue model on case studies of 2800TEU and 4400TEU container vessels, Journal of engineering for the Maritime Environment, Vol. 226(3), pp.222-234.

Mao, W. (2014). Development of a spectral method and a statistical wave model for crack propagation prediction in ship structures, Journal of Ship Research, Vol. 58(2), pp.106-116.

Mao, W., Rychlik, I. Wallin, J. and Storhaug, G. (2016). Statistical models for the speed prediction of a container ship, Ocean engineering, Vol. 126, pp 152-162.

Mao, W. and Rychlik, I. (2016). Probabilistic model for wind speed variability encountered by a vessel, Journal of engineering for the Maritime Environment, Vol. 5(13), pp. 837-855.

Marie, S. and Courteille, E. (2009). Multi-objective optimization of motor vessel route, International Navigational Symposium on Marine Navigation and Safety of Sea Transportation, Vol. 3(2), pp. 411-419, Gdynia, Poland.

OECD. (2015). The impact of mega-ships. https://www.itf-oecd.org/sites/default/files/docs/15cspa_mega-ships.pdf. [Accessed: 2020-03-14.]

Olsen, A.S., Schrøter, C. and Jensen, J.J. (2005). Wave height distribution observed by ships in the north atlantic, Journal of Ships and Offshore Structures, Vol. 1, pp. 1-12.

Osyczka, A. and Kundu, S. (1995). A new method to solve generalized multicriteria optimization problems using the simple genetic algorithm, Structural Optimization, Vol. 10(2), pp. 94-99.

Paris, P.C. and Erdogan, F. (1963). A critical analysis of crack propagation laws, Journal of Basic Engineering, Vol. 85(4), pp. 528–534.

Paris, P.C., Gomez, M.P. and Anderson, W.E. (1961). A rational analytic theory of fatigue, The Trend in Engineering, Vol. 13, pp. 9-14.

Padhy, C.P., Sen, D. and Bhaskaran, P.K. (2008). Application of wave model for weather routing of ships in the north Indian Ocean, Natural Hazards, Vol. 44, pp. 373-385.

Raaschou–Nielsen, O., Andersen, Z.J., Hvidberg, M., Jensen, S.S., Ketzel, M., Sørensen, M., et al. (2011). Air pollution from traffic and cancer incidence: a Danish cohort study, Environmental Health, Vol.10(1), pp. 67.

Roh, M. (2013). Determination of an economical shipping route considering the effects for sea state for lower fuel consumption, International Journal of Naval Architecture and Ocean Engineering, Vol.5(2), pp. 246-262.

Skoglund, L., Kuttenkeuler, J. and Rosen, A. (2012). A new method for robust route optimization in ensemble weather forecasts, KTH Aeronautical and Vehicle Engineering, Trita-AVE 2012:67.

Smith, T. W. P., Raucci, C., Hosseinloo, S. H., Rojon, I., Calleya, J., De La Fuente, S. S., Wu, P., and Palmer, K. (2016). CO2 emissions from international shipping: Possible reduction targets and their associated pathways, UMAS, London.

Storm Geo. (2020). http://www.stormgeo.com/.[Accessed: 2020-03-14.]

Sumi, Y. and Wang, Z.N. (1998). A finite-element simulation method for a system of growing cracks in a heterogeneous material, Mechanics of Materials, Vol 28(1–4), pp. 197-206.

Swift, A. (1993). Bridge Team Management, The Nautical Institute, London.

Shao, W. and Zhou, P. (2012). Development of a 3D dynamic programming method for weather routing, International Journal on Marine Navigation and Safety of Sea Transportation, Vol. 6(1), pp. 79-85.

Szłapczynska, J. and Smierzchalski, R. (2009). Multicriteria optimisation in weather routing, International Journal on Marine Navigation and Safety of Sea Transportation, Vol.3(4), pp.393-400

Tillig, F., Ringsberg, J.W, Mao. W. and Ramne. B. (2017). A generic energy systems model for efficient ship design and operation, Proceedings of the Institution of Mechanical Engineers, Part M: Journal of Engineering for the Maritime Environment, Vol. 231(2), pp. 649–666.

Tso, M.C. and Cheng, H.C. (2013). An ant colony algorithm for efficient ship routing, Polish maritime research, 3(79) 2013 Vol 20, pp. 28-38.

UNCTAD. (2019). Review of Maritime Transport 2019. https://unctad.org/en/pages/PublicationWebflyer.aspx?publicationid=2563. [Accessed: 2020-03-14.]

Veneti, A., Makrygiorgos, A., Konstantopoulos, C., et al. (2017). Minimizing the fuel consumption and the risk in maritime transportation: A bi-objective weather routing approach, Computers and Operations Research, Vol.88, pp.220-236.

Vettor, R. and Soares, C. G. (2016). Development of a ship weather routing system, Ocean Engineering, Vol. 123, pp. 1-14.

Wang, H. (2018). Voyage optimization algorithms for ship safety and energy-efficiency. Licentiate thesis, Chalmers University of Technology, Gothenburg, Sweden.

Wang, H., Li, X., Li, P., et al. (2018). Application of Real-Coded Genetic Algorithm in Ship Weather Routing, Journal of Navigation, Vol. 71(4), pp. 989-1010.

Wang, H., Mao, W., and Eriksson, L. E. (2017). Benchmark study of five optimization algorithms for weather routing, Proceedings of the ASME 2017 36th International Conference on Ocean, Offshore and Arctic Engineering, Trondheim, Norway, June 25-30, 2017.

Wang, H., Mao, W., Eriksson, L. E. (2018). Voyage optimization for mitigating ship structural failure due to crack propagation, Part O: Journal of Risk and Reliability, Vol. 233(1), pp. 5-17.

Wang, H., Mao, W,. Eriksson, L. E. (2018). Metocean data drived voyage optimization using genetic algorithm, Proceeding of the 28th ISOPE, Sapporo, Japan.

Wang, H., Mao, W., and Eriksson, L. (2019). A three-dimensional Dijkstra's algorithm for multi-objective ship voyage optimization, Ocean Engineering, Vol.186, 106131.

Wawrzynek, P. A., and Ingraffea, A. R. (1991), Discrete modelling of crack propagation: Theoretical aspects and implementation issues in two and three dimensions, Rep. 91-5, Sch. of Civ. and Environ. Eng., Cornell Univ., Ithaca, N. Y.

WNI weather routing. (2020). https://global.weathernews.com/your-industry/shipping/. [Accessed: 2020-03-14.]

Zaccone, R. and Figari, M. (2017). Energy efficient ship voyage planning by 3D dynamic programming, Journal of Ocean Technology, Vol.12(4), pp.49-71.

Zaccone, R., Ottaviani, E., Figari, M. and Altosole, M. (2018). Ship voyage optimization for safe and energy-efficient navigation: A dynamic programming approach. Ocean engineering, Vol. 153, pp. 215-224.